

On the Probability of Necessity and Sufficiency of Explaining Graph Neural Networks: A Lower Bound Optimization Approach

Ruichu Cai^{a,b}, Yuxuan Zhu^{a,*}, Xuexin Chen^a, Yuan Fang^c, Min Wu^d, Jie Qiao^{a,b}, Zhifeng Hao^e

^a*School of Computer Science, Guangdong University of Technology, Guangzhou 510006, China*

^b*Peng Cheng Laboratory, Shenzhen 518066, China*

^c*School of Computing and Information Systems, Singapore Management University, 178902, Singapore*

^d*Institute for Infocomm Research (I²R), A*STAR, 138632, Singapore*

^e*College of Science, Shantou University, Shantou 515063, China*

Abstract

The explainability of Graph Neural Networks (GNNs) is critical to various GNN applications, yet it remains a significant challenge. A convincing explanation should be both necessary and sufficient simultaneously. However, existing GNN explaining approaches focus on only one of the two aspects, necessity or sufficiency, or a heuristic trade-off between the two. Theoretically, the Probability of Necessity and Sufficiency (PNS) holds the potential to identify the most necessary and sufficient explanation since it can mathematically quantify the necessity and sufficiency of an explanation. Nevertheless, the difficulty of obtaining PNS due to non-monotonicity and the challenge of counterfactual estimation limit its wide use. To address the non-identifiability of PNS, we resort to a lower bound of PNS that can be optimized via counterfactual estimation, and propose a framework of Necessary and Sufficient Explanation for GNN (NSEG) via optimizing that lower bound. Specifically, we depict the GNN as a structural causal model (SCM), and estimate the probability of counterfactual via the intervention under the SCM. Additionally, we leverage continuous masks with a sampling strategy to optimize the lower bound to enhance the scalability. Empirical results demonstrate that NSEG outperforms state-of-the-art methods,

*This research was supported in part by National Key R&D Program of China (2021ZD0111501), National Science Fund for Excellent Young Scholars (62122022), Natural Science Foundation of China (61876043, 61976052, 62206064), the major key project of PCL (PCL2021A12).

*Corresponding author

Email addresses: cairuichu@gmail.com (Ruichu Cai), iamyuxuanzhu@gmail.com (Yuxuan Zhu), im.chenxuexin@gmail.com (Xuexin Chen), yfang@smu.edu.sg (Yuan Fang), wumin@i2r.a-star.edu.sg (Min Wu), qiaojie.chn@gmail.com (Jie Qiao), haozhifeng@stu.edu.cn (Zhifeng Hao)

consistently generating the most necessary and sufficient explanations.

Keywords:

Explainability, Graph Neural Networks, Causality, Explainable AI, Interpretability

1. Introduction

Graph Neural Networks (GNNs) differentiate themselves from neural networks designed for Euclidean data by not only learning feature information but also capturing graph structures through the message-passing mechanism [20, 15, 50, 44, 56, 21, 14, 48, 7]. This unique characteristic has facilitated the successful application of GNNs in various domains, including social recommendation [12, 16], molecule discovery [39, 40], and fraud detection [49, 11]. However, GNNs with high complexity are still considered black-box models [3, 30], which limits their applications in many real-life related domains like medicine and healthcare [34]. Although numerous studies have been proposed to explain neural networks for Euclidean data [36, 26, 41, 18], such approaches usually are not suitable for GNNs as they cannot explain the graph structures well. Hence, the explainability of GNNs remains an open challenge.

Current approaches for explaining GNNs mainly search for three types of explanation, i.e., necessary explanation, sufficient explanation, and the heuristic trade-off explanation between necessity and sufficiency. First, the approaches [23, 46, 25] searching for a necessary explanation seek to identify a group of necessary features that will change the prediction if one performs a perturbation. Although necessity is important for the explanation, the lack of sufficiency can result in the incompleteness of the explanations. For instance, consider a chat group classification task in which the hobby and social connections of each member are provided and we aim to explain why the instance given in Figure 1 is predicted as “Sport Lover Group”. For the necessary explanation shown on the top-right of Figure 1, only a small set of soccer lovers or basketball lovers are considered as explanations. However, it is insufficient as some basketball lovers are missing. In contrast, the approaches [52, 27] searching for a sufficient explanation seek to locate a subset of the graph that can sufficiently cause the outcome by maximizing the mutual information between the input and outcome. For such approaches, the sufficient explanation might not be concise enough for people to understand, e.g., in the bottom-left of Figure 1, the explanation covers almost the whole graph including both sports and snack lovers and their relationships. Furthermore, a recent approach [42] considers a trade-off between necessity and sufficiency, whereas the trade-off is heuristically determined by hyper-parameters so that the explanation obtained might not be the *most* necessary and sufficient.

Different from either sufficient or necessary explanations, a both necessary and sufficient explanation offers completeness without sacrificing conciseness. As illustrated in the bottom-right of Figure 1, the most necessary and sufficient

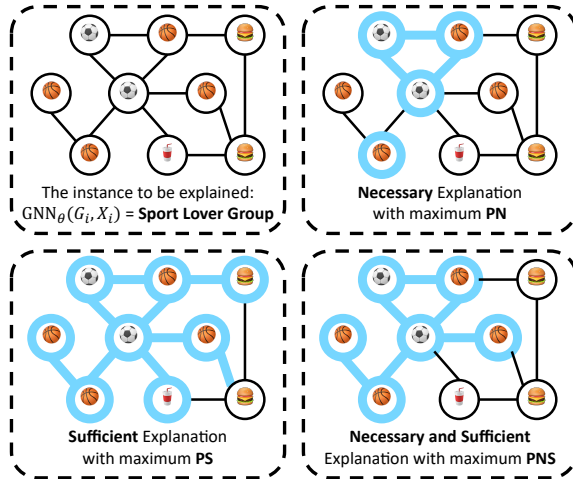


Figure 1: Explanations for the prediction “Sport Lover Group”, which are highlighted in blue. Each node is a member in the group whose node features are their hobby, denoted by the icons. PN, PS, PNS refer to the probability of necessity, the probability of sufficiency, and the probability of necessity and sufficiency, respectively.

explanation includes all sport lovers, ensuring completeness, while excluding the redundant snack lovers, ensuring conciseness. The necessity and sufficiency of the explanation deserve a privileged position in the theory and practice of explainable AI [47, 32], and we argue that *an ideal explanation should be most necessary and sufficient*. A formal way to quantify the necessity and sufficiency of an explanation is through the use of the *Probability of Necessity and Sufficiency* (PNS) [33]. However, there are two main challenges in identifying PNS: 1) the violation of the assumption of monotonicity making PNS not identifiable [32, 43] and 2) the difficulty of counterfactual estimation. On one hand, to address the above identifiability issue of PNS, we derive a lower bound of PNS that can be estimated via counterfactual estimation. On the other hand, for counterfactual estimation, we depict the GNN as a structural causal model (SCM) and estimate the counterfactual probability by intervention under the SCM. In addition, to enable tractable optimization, continuous masks with a sampling strategy are used to optimize the lower bound of PNS. By combining these techniques, we propose a framework of **Necessary and Sufficient Explanation for GNNs** (NSEG), via maximizing the lower bound of PNS.

Our contributions can be summarized as follows:

- We propose NSEG to generate necessary and sufficient explanations for GNNs, by optimizing a lower bound of PNS via counterfactual estimation.
- We depict the GNN as an SCM such that the counterfactual estimation is tractable via intervention on the SCM. We further leverage a continuous mask with a sampling strategy to optimize the lower bound of PNS,

making the optimization tractable by relaxing the discrete explanation to a continuous case.

- Our experiments show that the explanations from NSEG are the most necessary and sufficient, and both aspects are critical to the generation of explanations.

2. Related Work

2.1. Graph Neural Networks

Graph Neural Networks (GNNs) [20, 15, 50, 44, 56, 21, 14, 48, 7, 9, 55, 24, 10] have demonstrated tremendous success in various real-world applications, e.g., social recommendation [12, 16], molecule discovery [39], etc. Inspired by Convolutional Neural Networks (CNN) [22], graph convolution is applied in graph data to make the networks more efficient and convenient. Over the years, various convolutional GNNs have been proposed, including spectral-based and spatial-based approaches. Graph Convolutional Networks (GCN) later bridge the gap between spectral-based approaches and spatial-based [20], and then spatial-based approaches become more popular as they are efficient, flexible and general. For example, GraphSAGE with its proposed sampling and aggregation strategies [15] can be used for inductive learning and large-scale graph learning. Graph Attention Networks (GAT) adopt the self-attention mechanism to differentiate the importance of neighbors [44]. Graph Isomorphism Networks (GIN) introduce a pooling architecture so that they have expressive power as Weisfeiler-Lehman test [50].

2.2. GNN Explaining Approaches

Most of the GNN explanation approaches can be categorized into four types: perturbation-based, gradient-based, decomposition, and surrogate approaches [53].

Our proposed approach is closely aligned with perturbation-based methods, which study the outcome changes w.r.t. different input perturbations. GNNExpainer [52] employs a trainable mask to perturb the data in the input space, to maximize the mutual information between perturbed input data and model outcome, to obtain a subgraph explanation that is relevant for the particular prediction. Though PGExpainer [27] shares the same objective with GNNExpainer, it achieved faster inference time by learning a parameterized mapping from the graph representation space to subgraph space. CF-GNNExpainer generates a counterfactual explanation that can flip the model prediction subject to a minimal perturbation [25]. RG-Expainer [38] leverages Reinforcement Learning (RL) algorithm to generate the explanation by sequentially adding nodes (action) based on the current generated explanation (state), which has the similar objective (reward) with [27]. RC-Expainer [46] also employs a RL algorithm to search for the explanation that maximizes the causal effect obtained by the edge perturbation. CF² [42], arguably the most closely related work to our approach, utilizes both factual and counterfactual reasoning to generate heuristic

necessary and sufficient explanations. The main difference between CF^2 and ours is that the former searches for a trade-off explanation between necessity and sufficiency, while our work searches for the most necessary and sufficiency explanation. Besides, CF^2 only samples one counterfactual (necessary) for computing the necessary strength, which is a degradation to ours.

Gradient-based approaches approximate the importance of an input using the gradients of its outcome obtained by back-propagation. The saliency map approach, which is used to indicate the input importance, is obtained by computing the squared norm of the gradients [4]. In another method called Guided Backpropagation (GBP), the negative gradients are clipped during back-propagation as negative gradients are challenging to explain [4].

Decomposition approaches aim to decompose the model outcome into several terms as the importance scores of the corresponding input feature. Layer-wise Relevance Propagation (LRP) decomposes the GNN output into node importance scores, whereas the edge importance scores cannot be provided [4]. EBP [35] shares a similar idea with LRP, while it is based on the law of total probability.

Surrogate approaches leverage a simple and interpretable model to approximate the behavior of a complex model locally. GraphLIME [17] extends the LIME algorithm [36], and employs a Hilbert-Schmidt Independence Criterion Lasso as a surrogate to approximate the GNN instance. In particular, the weights of the surrogate model indicate the importance scores of the nodes. In PGM-Explainer [45], a probabilistic graphical model is utilized as surrogate for explaining the GNN instance.

2.3. Casual Explainability

Causal inference has a long history in statistics [33] and there is now an increasing interest in solving crucial problems of machine learning that benefit from causality [37, 51, 58, 5], including explainability. The well-known perturbation-based approaches such as LIME [36], Shapley values [26] implicitly use causal inference to estimate the attribution scores, which can be viewed as a special case of causal effect. Besides, Chattopadhyay et al. [8] views the neural network architecture as a Structural Causal Model (SCM) and estimates the average causal effect upon it. Also, there are a few works [47, 13, 57, 6] utilizing the aspects of necessity and sufficiency for explainability via causal interpretations, which are the most related works to ours.

3. Preliminary

3.1. Causality

Since the probability of necessity and sufficiency (PNS), the probability of necessity (PN), and the probability of sufficiency (PS), are rigorously defined in the language of causality [33, 32, 43], here we introduce the basic causality preliminaries to enhance the understanding of this work. The identification of PNS, PN, and PS requires the counterfactual estimation. In the literature

of [33], counterfactual is obtained by intervention under the structural causal model (SCM), which is defined in Definition 1.

Definition 1. (*Structural Causal Model*). A structural causal model is a triplet:

$$M = (\mathbf{U}, \mathbf{V}, F),$$

where

1. \mathbf{U} is a set of variables called exogenous, that are determined by factors outside the model.
2. \mathbf{V} is a set of variables called endogenous, that are determined by variables in the model, i.e., $\mathbf{U} \cup \mathbf{V}$.
3. F is a set of functions where each f_i is a mapping from $\mathbf{U} \times (\mathbf{V} \setminus \mathbf{v}_i)$ to \mathbf{v}_i , i.e.,

$$\mathbf{v}_i = f_i(Pa(\mathbf{v}_i), \mathbf{u}_i),$$

where $Pa(\mathbf{V}_i)$ are the parent variables of \mathbf{v}_i , and \mathbf{u}_i is the exogenous of \mathbf{v}_i .

A SCM can properly model the data-generating process through functional mechanisms, that is, an endogenous \mathbf{V}_i is determined by its parents $Pa(\mathbf{v}_i)$ and exogenous \mathbf{u}_i via the function f_i , denoted as $\mathbf{v}_i = f_i(Pa(\mathbf{v}_i), \mathbf{u}_i)$. The functional characterization in SCM provides a convenient language for specifying how the resulting distribution would change in response to interventions. The simplest intervention, such as an intervention of $do(\mathbf{v}_i = v'_i)$, amounts to removing the old generating mechanism $\mathbf{v}_i = f_i(Pa(\mathbf{v}_i), \mathbf{u}_i)$ from the SCM and substituting $\mathbf{v}_i = v'_i$ in the remaining generating equations.

The concept of counterfactual refers to the consequences of the interventions, given certain facts. In particular, the given certain facts provide evidence about the actual state of the world, which is exogenous in the literature of [33]. The counterfactual is obtained by intervening on some variables under the SCM while keeping the actual state (exogenous) the same.

3.2. Graph Neural Networks

Graph neural networks are capable of incorporating both graph structure and node features into representations in an end-to-end fashion, to facilitate downstream tasks such as node classification task and graph classification task. In particular, in the k -th layer of GNNs, the learning process of the representation of node v can be divided into the following three steps:

- First, obtaining message $\mathbf{m}_{v,u}^{(k)}$ for any node pair (v, u) through a message function MSG :

$$\mathbf{m}_{v,u}^{(k)} = MSG(\mathbf{h}_v^{(k-1)}, \mathbf{h}_u^{(k-1)}, \mathbf{e}_{v,u}),$$

where $\mathbf{h}_v^{(k-1)}$ and $\mathbf{h}_u^{(k-1)}$ denote the representations of nodes v and u in the $(k-1)$ -th layer, and $\mathbf{e}_{v,u}$ denotes the entry (relation) between nodes v and u .

- Second, aggregating messages from node v 's neighbors \mathcal{N}_v and calculating the an aggregated message $\mathbf{M}_v^{(k)}$ via a aggregating function AGG :

$$\mathbf{M}_v^{(k)} = AGG(\mathbf{m}_{v,u}^{(k)} | u \in \mathcal{N}_v).$$

- Third, updating node v 's representation $\mathbf{h}_v^{(k)}$ using the aggregated messages $\mathbf{M}_v^{(k)}$ and node v 's representation in the previous layer $\mathbf{h}_v^{(k-1)}$ via a update function $UPDATE$:

$$\mathbf{M}_v^{(k)} = UPDATE(\mathbf{M}_v^{(k)}, \mathbf{h}_v^{(k-1)}).$$

After obtaining the representation of each node, a node-level read-out and a graph-level read-out can be applied for node classification task and graph classification task respectively.

3.3. Problem Definition

Given a trained GNN model f_θ parameterized by θ for graph classification task, our task is to explain a specific instance $\mathcal{I} : \hat{y} = f_\theta(E_i, X_i)$ produced by the model f_θ by generating a necessary and sufficient explanation in a post-hoc manner, where \hat{y} is the predicted label, $X_i = \{x_v | v \in V_i\}$, and E_i, X_i are edges and vertices of graph G_i . In our framework, we consider the explanation of a specific instance \mathcal{I} as an event, i.e., $(\mathbf{E} = E'_i, \mathbf{X} = X'_i)$, that most necessarily and sufficiently causes the model outcome $\mathbf{Y} = \hat{y}$ (with maximum PNS), where $E'_i \subset E_i$ and $X'_i = \{x_v | v \in V'_i\}$ with $V'_i \subset V_i$. Note that our main focus is to identify a set of node features instead of a set of features in the feature dimensions, where the latter has been well investigated in [8]. Similarly, as for the formulation of node classification task, our task is to explain a node-level instance $\mathcal{I} : \hat{y}_i = f_\theta^{(i)}(E, X)$ for node i by generating a necessary and sufficient explanation $\mathbf{E} = E', \mathbf{X} = X'$, where \hat{y}_i is the predicted label of node i . Without loss of generality, we formulate our approach in a graph classification fashion in the following paper. Regarding our notations, we use the bold font notation for random variable to emphasize the distinction between r.v. and its realization.

4. Methodology

In this section, we develop our approach NSEG to generate the most **N**ecessary and **S**ufficient **E**xplanations for **G**NNs by optimizing our objective, the **P**robability of **N**ecessity and **S**ufficiency (PNS). We maximize a derived lower bound of PNS since the non-identifiability of PNS and incorporate a proposed SCM of GNN for the identification of the lower bound. Additionally, we introduce a continuous optimization method that utilizes continuous masks and a sampling strategy. This approach enables tractable optimization of large-scale graphs, ensuring the scalability and efficiency of our approach.

4.1. Lower Bound of the Explanation's PNS

As we discussed before, a convincing explanation should be necessary and sufficient. To quantify the degree of necessity and sufficiency of an explanation to the model outcome, the Probability of Necessity and Sufficiency (PNS) is introduced. Formally, to search for the most necessary and sufficient explanation (denoted as ξ) to the model outcome (denoted as \hat{y}), our objective is to maximize PNS w.r.t. ξ :

$$\max_{\xi \in \Xi} \text{PNS}(\xi), \quad (1)$$

where Ξ is the explanation space. In essence, the explanation with the highest PNS value can be considered the most necessary and sufficient for the model outcome. The formal definition of PNS is as follows.

Definition 2. (*Probability of necessity and sufficiency of the explanation*).

$$\text{PNS}(\xi) = P(\mathbf{Y}_{\xi^c} \neq \hat{y}, \mathbf{Y}_{\xi} = \hat{y}), \quad (2)$$

where \mathbf{Y}_{ξ^c} and \mathbf{Y}_{ξ} are the potential outcome variables under the treatments ξ^c and ξ respectively, and ξ^c is the complementary event of ξ .

PNS measures the necessity and sufficiency of treatment ξ to model outcome \hat{y} in probability space. Intuitively, PNS indicates the probability that the outcome \hat{y} responds to both treatments ξ and ξ^c . However, direct optimization of the objective is intractable, given the non-identifiability of PNS shown in Eq. (2) due to the potential violation of monotonicity as defined in Definition 3, as well as the challenges of counterfactual estimation [33].

Definition 3. (*Monotonicity*). *The model outcome \mathbf{Y} is monotonic relative to the explanation event ξ if and only if:*

$$(\mathbf{Y}_{\xi} \neq \hat{y}) \wedge (\mathbf{Y}_{\xi^c} = \hat{y}) = \text{false}.$$

Monotonicity indicates that a change from ξ^c to ξ cannot assure the outcome also changes from $\mathbf{Y} = \hat{y}$ to $\mathbf{Y} \neq \hat{y}$ [32]. However, the assumption of monotonicity will not always hold during the explanation searching stage. Instead of addressing the non-monotonic issue to identify the exact PNS, it is reasonable to maximize a lower bound of $\text{PNS}(\xi)$ as shown in Lemma 1 for our objective optimization.

Lemma 1. *The lower bound of $\text{PNS}(\xi)$ is:*

$$\max\{0, P(\mathbf{Y}_{\xi^c} \neq \hat{y}) + P(\mathbf{Y}_{\xi} = \hat{y}) - 1\}. \quad (3)$$

In particular, the lower bound is tight if the assumption of monotonicity holds, as shown in Lemma 2. The proof of Lemma 2 is given in Appendix A.2.

Lemma 2. *When the outcome \mathbf{Y} is monotonic relative to explanation event ξ , the lower bound in Eq. (3) equals to the exact $\text{PNS}(\xi)$.*

Although PNS has been formally defined, applying it to GNNs is not a straightforward task due to: 1) the combined influence of both structural information (edges) and feature information (node features) on GNN predictions, 2) GNN takes continuous inputs rather than a binary event ξ . To overcome these challenges, we extend PNS to the graph domain by defining a joint binary event $(\mathbf{E} = E'_i, \mathbf{X} = X'_i)$ as the explanation, and its complement event $(\mathbf{E} = E'_i, \mathbf{X} = X'_i)^c$ which can be derived as $(\mathbf{E} \neq E'_i, \mathbf{X} \neq X'_i) \vee (\mathbf{E} \neq E'_i, \mathbf{X} = X'_i) \vee (\mathbf{E} = E'_i, \mathbf{X} \neq X'_i)$. Hence, our objective becomes maximizing the probability of necessity and sufficiency w.r.t. E'_i and X'_i as:

$$\max_{E'_i, X'_i} \text{PNS}^{e,f}(E'_i, X'_i), \quad (4)$$

where $\text{PNS}^{e,f}(E'_i, X'_i)$ is defined as:

$$\begin{aligned} & \text{PNS}^{e,f}(E'_i, X'_i) \\ &= P_\theta(\mathbf{Y}_{(\mathbf{E}=E'_i, \mathbf{X}=X'_i)^c} \neq \hat{y}, \mathbf{Y}_{\mathbf{E}=E'_i, \mathbf{X}=X'_i} = \hat{y}), \end{aligned} \quad (5)$$

where θ denotes the model parameter. The lower bound of $\text{PNS}^{e,f}(E'_i, X'_i)$ is:

$$\begin{aligned} & \max\{0, P_\theta(\mathbf{Y}_{(\mathbf{E}=E'_i, \mathbf{X}=X'_i)^c} \neq \hat{y}) \\ & \quad + P_\theta(\mathbf{Y}_{\mathbf{E}=E'_i, \mathbf{X}=X'_i} = \hat{y}) - 1\}. \end{aligned} \quad (6)$$

Note that our approach to optimize the above lower bound in Eq. (6) provides a joint explanation of both the edge and node feature. Single edge explanation and single node feature explanation are special cases of our joint explanation. Specifically, the formulations of single-edge and single-node features are familiar with the joint formulation, which are given by:

$$\begin{aligned} \text{PNS}^e(E'_i, X_i) &= P_\theta(\mathbf{Y}_{\mathbf{E} \neq E'_i} \neq \hat{y}, \mathbf{Y}_{\mathbf{E}=E'_i} = \hat{y} | \mathbf{X} = X_i), \\ \text{PNS}^f(E_i, X'_i) &= P_\theta(\mathbf{Y}_{\mathbf{X} \neq X'_i} \neq \hat{y}, \mathbf{Y}_{\mathbf{X}=X'_i} = \hat{y} | \mathbf{E} = E_i), \end{aligned}$$

where the lower bound of each is shown as follows respectively.

$$\begin{aligned} & \max\{0, P_\theta(\mathbf{Y}_{\mathbf{E}=E'_i} \neq \hat{y} | X_i) + P_\theta(\mathbf{Y}_{\mathbf{E}=E'_i} = \hat{y} | X_i) - 1\}, \\ & \max\{0, P_\theta(\mathbf{Y}_{\mathbf{X}=X'_i} \neq \hat{y} | E_i) + P_\theta(\mathbf{Y}_{\mathbf{X}=X'_i} = \hat{y} | E_i) - 1\}. \end{aligned}$$

4.2. Estimating the Lower Bound via Counterfactual Estimation

4.2.1. GNN as Structural Causal Model

The potential outcome term in Eq. (6) can be obtained by generating counterfactual by intervention under a specific structural causal model (SCM) [33]. In terms of counterfactual, it answers what will the outcome \mathbf{Y} be if $(\mathbf{E} = E'_i, \mathbf{X} = X'_i)^c$ or $(\mathbf{E} = E'_i, \mathbf{X} = X'_i)$. Building upon the interpretation of feed-forward neural networks as SCM for investigating causal attribution [1, 8], we extend the SCM interpretation to GNNs. In particular, GNNs can be interpreted as directed acyclic graphs with directed edges from the lower layer to the layer above.

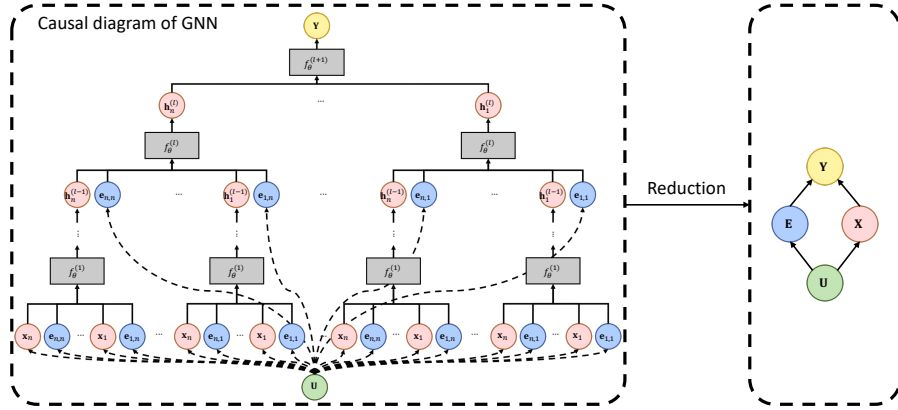


Figure 2: The causal diagram of corresponding SCM of GNN. \mathbf{h}_v^k denotes the hidden representation of node v in k -th layer, $\mathbf{e}_{v,u}$ denotes the entry between v and u , \mathbf{x}_v denotes the node feature of node v , $\mathbf{H}^{(k)} = \{\mathbf{h}_v^{(k)} | v \in V\}$ denotes a set of node representations in k -th layer, $\mathbf{X} = \{\mathbf{x}_v | v \in V\}$ denotes a set of node features, $\mathbf{E} = \{\mathbf{e}_{v,u} | v, u \in V\}$ denotes a set of graph entries.

Proposition 1. An $(l+1)$ -layer GNN corresponds to an SCM $M(\{\mathbf{X}, \mathbf{E}, \mathbf{H}^{(1)}, \dots, \mathbf{H}^{(l)}, \mathbf{Y}\}, \mathbf{U}, \{f_\theta^{(0)}, f_\theta^{(1)}, \dots, f_\theta^{(l+1)}\})$, where $\mathbf{H}^{(k)}$ denotes a set of node hidden representation after the k -th graph convolution layer, i.e., $\mathbf{H}^{(k)} = f_\theta^{(k)}(\mathbf{E}, \mathbf{H}^{(k-1)})$. $f_\theta^{(l+1)}$ denotes the read-out layer, which can be a node-level read-out for node classification tasks or a graph-level read-out for graph classification tasks, with $\mathbf{Y} = f_\theta^{(l+1)}(\mathbf{H}^{(l)})$. \mathbf{U} refers to a set of exogenous which act as causal factors for \mathbf{X} and \mathbf{E} , i.e., $\mathbf{E}, \mathbf{X} = f^{(0)}(\mathbf{U})$.

The proof of Proposition 1 is provided in Appendix A.3. For a more intuitive understanding, the left side of Figure 2 illustrates M 's corresponding causal diagram. In the k -th layer of GNN, the node v 's representation $\mathbf{h}_v^{(k)}$ is determined by all nodes' representations $\mathbf{H}^{(k-1)}$ in $(k-1)$ -th layer and the entry of the graph \mathbf{E} , specifically, aggregating node u 's representation $\mathbf{h}_u^{(k-1)}$ to obtain $\mathbf{h}_v^{(k)}$ if the entry $\mathbf{e}_{v,u}$ is not zero. Since our focus is on the mapping from the input to output rather than the full intrinsic mappings in the hidden layer, the SCM of GNN can be reduced to SCM $M(\{\mathbf{E}, \mathbf{X}, \mathbf{Y}\}, \mathbf{U}, \{f^{(0)}, f_\theta\})$ by marginalizing the hidden representations.

Proposition 2. The SCM of an $(l+1)$ -layer GNN, $M(\{\mathbf{X}, \mathbf{E}, \mathbf{H}^{(1)}, \dots, \mathbf{H}^{(l)}, \mathbf{Y}\}, \mathbf{U}, \{f^{(0)}, f_\theta^{(1)}, \dots, f_\theta^{(l+1)}\})$ can be reduced to $M(\{\mathbf{E}, \mathbf{X}, \mathbf{Y}\}, \mathbf{U}, \{f^{(0)}, f_\theta\})$.

The proof of Proposition 2 is presented in Appendix A.4. Intuitively, marginalizing the hidden representations is analogous to deleting edges connecting the hidden representations and creating new directed edges from the parents of the deleted to their respective child vertices in the causal diagram depicted on the left side of Figure 2. The corresponding causal diagram of the reduced SCM in Proposition 2 is shown on the right side of Figure 2.

4.2.2. Counterfactual Estimation

Given the reduced SCM depicted in Proposition 2, we can obtain the interventional probability via *do*-calculus, by controlling \mathbf{E} and \mathbf{X} for edges and node features respectively. To facilitate understanding, we present the formulations separately for edges and node features before combining them to give the joint formulation.

Counterfactual for Edges. Regarding edges, the interventional probability of the counterfactual ($\mathbf{E} = E'_i$) can be obtained by intervening on \mathbf{E} , i.e., replacing the causal mechanism from exogenous \mathbf{U} to the edge \mathbf{E} with the intervention $do(\mathbf{E} = E'_i)$ while keeping other mechanisms unperturbed, i.e., $\mathbf{X} = X_i$:

$$\begin{aligned} & P_\theta(\mathbf{Y}_{\mathbf{E}=E'_i} = \hat{y} | \mathbf{X} = X_i) \\ &= P_\theta(\mathbf{Y} = \hat{y} | do(\mathbf{E} = E'_i), \mathbf{X} = X_i) \\ &= f_\theta^{\hat{y}}(E'_i, X_i), \end{aligned} \tag{7}$$

where $f_\theta^{\hat{y}}(\cdot, \cdot)$ outputs the probability of the class \hat{y} . As for the interventional probability of the counterfactual ($\mathbf{E} \neq E'_i$),

$$\begin{aligned} & P_\theta(\mathbf{Y}_{\mathbf{E} \neq E'_i} \neq \hat{y} | \mathbf{X} = X_i) \\ &= P_\theta(\mathbf{Y} \neq \hat{y} | do(\mathbf{E} \neq E'_i), \mathbf{X} = X_i) \\ &= P_\theta(\mathbf{Y} \neq \hat{y} | \mathbf{E} \in \mathcal{E}_i \setminus E'_i, \mathbf{X} = X_i) \\ &= 1 - \mathbb{E}_{\overline{E}'_i} [f_\theta^{\hat{y}}(\overline{E}'_i, X_i)], \end{aligned} \tag{8}$$

where $\overline{E}'_i \sim p(\overline{E}'_i | \mathcal{E}_i \setminus E'_i)$ which can be specified by $p(\mathbf{U})$ according to the corresponding SCM, and \mathcal{E}_i is the sub-edge space of graph G_i . In the absence of any prior knowledge of $p(\overline{E}'_i | \mathcal{E}_i \setminus E'_i)$, it is reasonable to assume $p(\overline{E}'_i | \mathcal{E}_i \setminus E'_i)$ is uniformly distributed over the sub-edge space \mathcal{E} , which encourage the exploration of all ($\mathbf{E} \neq E'_i$). Prior knowledge $p(\mathbf{U})$ can also be incorporated to refine the estimation of counterfactual.

Counterfactual for Node Features. Our goal is to identify a subset of node features that cause the prediction, that is, features in a subset of nodes V'_i , instead of identifying a subset of feature in feature dimensions. One way to incorporate sub-node structure with the node features is to set the features outside V'_i to $\mathbf{0}$ while keeping features inside V'_i the same, since the zero-valued features have no impact in feed-forward process. Thus, the interventional probability of counterfactual ($\mathbf{X} = X'_i$) can be obtained by intervening on \mathbf{X} , i.e., replacing the causal mechanism from \mathbf{U} to \mathbf{X} with the intervention $do(\mathbf{X} = X'_i)$ while keeping other mechanisms unperturbed, which is given by,

$$\begin{aligned} & P_\theta(\mathbf{Y}_{\mathbf{X}=X'_i} = \hat{y} | \mathbf{E} = E_i) \\ &= P_\theta(\mathbf{Y} = \hat{y} | do(\mathbf{X} = X'_i), \mathbf{E} = E_i) \\ &= f_\theta^{\hat{y}}(E_i, X'_i) \\ & \text{with } X'_i = \{x_v | v \in V'_i\} \cup \{\mathbf{0} | v \notin V'_i\}. \end{aligned} \tag{9}$$

Likewise, the interventional probability of counterfactual ($\mathbf{X} = X'_i$) is given by

$$\begin{aligned}
& P_\theta(\mathbf{Y}_{\mathbf{X} \neq X'_i} \neq \hat{y} | \mathbf{E} = E_i) \\
&= P_\theta(\mathbf{Y} \neq \hat{y} | do(\mathbf{X} \neq X'_i), \mathbf{E} = E_i) \\
&= \mathbb{E}_{\bar{X}'_i} [P_\theta(\mathbf{Y} \neq \hat{y} | \mathbf{X} = \bar{X}'_i, \mathbf{E} = E_i)] \\
&= 1 - \mathbb{E}_{\bar{X}'_i} [f_\theta^{\hat{y}}(E_i, \bar{X}'_i)] \\
&\quad \text{with } \bar{X}'_i = \{x_v | v \in \bar{V}'_i\} \cup \{\mathbf{0} | v \notin \bar{V}'_i\},
\end{aligned} \tag{10}$$

where $\bar{X}'_i \sim p(\bar{X}'_i | \bar{V}'_i) p(\bar{V}'_i | \mathcal{V}_i \setminus V'_i) = p(\bar{V}'_i | \mathcal{V}_i \setminus V'_i)$, and \mathcal{V}_i is sub-node space of graph G_i .

Joint Formulation of Edge and Node Feature. The joint formulation of both edge and node feature explanation in Eq. (6) requires us to generate counterfactual for edge and node feature by intervention on both \mathbf{E} and \mathbf{X} . Notably, the event $(\mathbf{E} = E'_i, \mathbf{X} = X'_i)^c$ in Eq. (6) can be divided into three sub-events, $(\mathbf{E} \neq E'_i, \mathbf{X} \neq X'_i)$, $(\mathbf{E} \neq E'_i, \mathbf{X} = X'_i)$, and $(\mathbf{E} = E'_i, \mathbf{X} \neq X'_i)$. According to the interventional probability in Eqs. (7), (8), (9), and (10), the lower bound of PNS in Eq. (6) can be derived as follows.

$$\begin{aligned}
& \max\{0, -P_{00} \mathbb{E}_{\bar{E}'_i, \bar{X}'_i} [f_\theta^{\hat{y}}(\bar{E}'_i, \bar{X}'_i)] \\
& \quad - P_{01} \mathbb{E}_{\bar{E}'_i} [f_\theta^{\hat{y}}(\bar{E}'_i, X'_i)] \\
& \quad - P_{10} \mathbb{E}_{\bar{X}'_i} [f_\theta^{\hat{y}}(E'_i, \bar{X}'_i)] \\
& \quad + f_\theta^{\hat{y}}(E'_i, X'_i)\},
\end{aligned} \tag{11}$$

with:

$$\begin{aligned}
P_{00} &= P(\mathbf{E} \neq E'_i, \mathbf{X} \neq X'_i | (\mathbf{E} = E'_i, \mathbf{X} = X'_i)^c), \\
P_{01} &= P(\mathbf{E} \neq E'_i, \mathbf{X} = X'_i | (\mathbf{E} = E'_i, \mathbf{X} = X'_i)^c), \\
P_{10} &= P(\mathbf{E} = E'_i, \mathbf{X} \neq X'_i | (\mathbf{E} = E'_i, \mathbf{X} = X'_i)^c),
\end{aligned} \tag{12}$$

Without any prior knowledge regarding P_{00} , P_{01} , and P_{10} in Eq. (12), it is reasonable to assume $P_{00} = P_{01} = P_{10} = \frac{1}{3}$ for the encouragement of fair exploration of each case.

4.3. Generating the Explanation via Lower Bound Optimization

Continuous mask. Enumerating all possible E'_i and X'_i for objective optimization in large-scale graphs is infeasible. To enhance the scalability of our approach, we adopt a continuous relaxation approach, as in [52], using continuous masks that allow for optimization through gradient descent. In particular, we design two masks $M_e \in [0, 1]^m$ and $M_f \in [0, 1]^n$ to mask the edges E_i and the node feature X_i to obtain E'_i and X'_i respectively, where m is the number of edges, and n is the number of nodes. Intuitively, $M_e^k = 0$ indicates that deleting

the k -th edge from the full edges E_i , while $M_e^k = 1$ indicates retaining the k -th edge.

$$\begin{aligned} E'_i &= M_e \odot E_i, \\ X'_i &= M_f \odot X_i + (1 - M_f) \odot \mathbf{0} = M_f \odot X_i, \end{aligned}$$

where \odot denotes the Hadamard multiplication, and $\mathbf{0} \in 0^{n \times d}$ denotes a zero matrix. After masking, the term $f_\theta^{\hat{y}}(E'_i, X'_i)$ in Eq. (11) can be derived as follows.

$$f_\theta^{\hat{y}}(E'_i, X'_i) = f_\theta^{\hat{y}}(M_e \odot E_i, M_f \odot X_i), \quad (13)$$

Sampling strategy. Incorporating the masks to generate samples from $p(\overline{E}'_i | \mathcal{E}_i \setminus E'_i)$ and $p(\overline{V}'_i | \mathcal{V}_i \setminus V'_i)$ in Eq. (11), a heuristic sampling strategy is proposed such that the Monte Carlo estimation of the expectations in Eq. (11) are differentiable w.r.t. M_e and M_f . Inspired by the reparameterization trick proposed in [19], an auxiliary variable ϵ is used in our sampling strategy for the sample generation.

Specifically, the generating process of edge sample \overline{E}'_i from $p(\overline{E}'_i | \mathcal{E}_i \setminus E'_i)$ can be expressed as a deterministic function with auxiliary variable ϵ_e , which is:

$$\overline{E}'_i = (1 - M_e + \epsilon_e) \odot E_i, \quad \epsilon_e \sim p(\epsilon_e). \quad (14)$$

Intuitively, the term $1 - M_e$ aims to satisfy the given condition of $\mathbf{E} \in \mathcal{E}_i \setminus E'_i$, and a positive value of ϵ_e^k increases the weight of the existence of the k -th edge, while a negative value decreases the weight. Without any prior knowledge of $p(\overline{E}'_i | \mathcal{E}_i \setminus E'_i)$, it is reasonable to assume ϵ_e is uniformly distributed to encourage the fair exploration. Similarly, the generating process of node feature sample \overline{X}'_i from $p(\overline{V}'_i | \mathcal{V}_i \setminus V'_i)$ can be expressed as follows.

$$\overline{X}'_i = (1 - M_f + \epsilon_f) \odot X_i, \quad \epsilon_f \sim p(\epsilon_f). \quad (15)$$

Thus, combining with Eqs. (14) and (15) the term $\mathbb{E}_{\overline{E}'_i, \overline{X}'_i} [f_\theta^{\hat{y}}(\overline{E}'_i, \overline{X}'_i)]$ in Eq. (11) can be derived as:

$$\mathbb{E}_{\epsilon_e, \epsilon_f} [f_\theta^{\hat{y}}((1 - M_e + \epsilon_e) \odot E_i, (1 - M_f + \epsilon_f) \odot X_i)], \quad (16)$$

similarly, the term $\mathbb{E}_{\overline{E}'_i} [f_\theta^{\hat{y}}(\overline{E}'_i, X'_i)]$ is given by:

$$\mathbb{E}_{\epsilon_e} [f_\theta^{\hat{y}}((1 - M_e + \epsilon_e) \odot E_i, M_f \odot X_i)], \quad (17)$$

also, the term $\mathbb{E}_{\overline{X}'_i} [f_\theta^{\hat{y}}(E'_i, \overline{X}'_i)]$ is given by:

$$\mathbb{E}_{\epsilon_f} [f_\theta^{\hat{y}}(M_e \odot E_i, (1 - M_f + \epsilon_f) \odot X_i)]. \quad (18)$$

Overall, the final optimizable lower bound of PNS combined with continuous masks, $\text{PNS}_{lb}^{e,f}$, is given as follows.

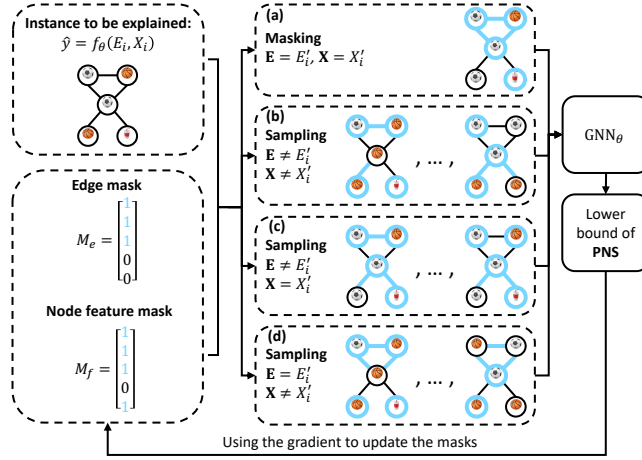


Figure 3: Illustration of the overall framework of NSEG. (a) is the process to obtain Eq. (13); (b), (c), and (d) are the processes to obtain Eqs. (16), (17), and (18), respectively.

$$\begin{aligned}
& \max\{0, -P_{00}\mathbb{E}_{\epsilon_e, \epsilon_f}[f_{\theta}^{\hat{y}}((1 - M_e + \epsilon_e) \odot E_i, (1 - M_f + \epsilon_f) \odot X_i)] \\
& \quad - P_{01}\mathbb{E}_{\epsilon_e}[f_{\theta}^{\hat{y}}((1 - M_e + \epsilon_e) \odot E_i, M_f \odot X_i)] \\
& \quad - P_{10}\mathbb{E}_{\epsilon_f}[f_{\theta}^{\hat{y}}(M_e \odot E_i, (1 - M_f + \epsilon_f) \odot X_i)] \\
& \quad + f_{\theta}^{\hat{y}}(M_e \odot E_i, M_f \odot X_i)\},
\end{aligned} \tag{19}$$

Despite joint explanation, for single edge explanation, the final objective is $\max\{0, \mathbb{E}_{\epsilon_e}[-f_{\theta}^{\hat{y}}((1 - M_e + \epsilon_e) \odot E_i, X_i)] + f_{\theta}^{\hat{y}}(M_e \odot E_i, X_i)\}$. Similarly for single node feature explanation, the final objective is $\max\{0, \mathbb{E}_{\epsilon_f}[f_{\theta}^{\hat{y}}(E_i, (1 - M_f + \epsilon_f) \odot X_i)] + f_{\theta}^{\hat{y}}(E_i, M_f \odot X_i)\}$.

4.4. Model Summary

The overall framework of NSEG is depicted in Figure 3. To explain an instance $\mathcal{I} : \hat{y} = f_{\theta}(E_i, X_i)$, an edge mask M_e and a node feature mask M_f are used to obtain and maximize the lower bound of PNS in Eq. (19). Then the gradients of the overall loss w.r.t. to the masks are employed to update the masks and obtain the necessary and sufficient explanation. Specifically, we utilize a *mask size* regularization term to enhance the optimization, which is also adopted in prior works [52, 27]. Intuitively, the regularization operates as an L_1 penalization, compelling the explanation to concentrate on the most important portions of the input. Besides, a *mask entropy* regularization term is added to discretize the mask, i.e., the values of the mask are concentrated around a few scalars when the *mask entropy* is low [2]. Formally, the overall loss \mathcal{L} is:

$$\mathcal{L} = -\text{PNS}_{lb} + \alpha_e \|M_e\|_1 + \beta_e \text{Ent}(M_e) + \alpha_f \|M_f\|_1 + \beta_f \text{Ent}(M_f), \tag{20}$$

where PNS_{lb} is the lower bound of PNS shown in Eq. (19), and $\text{Ent}()$ is the element-wise entropy to encourage the discretization of the mask.

Formally, the NSEG algorithm is outlined in Algorithm 1. After obtaining the final masks M_e and M_f , the explanation (E'_i, X'_i) can be obtained via *extract_explanation* in Algorithm 1. The possible choices for *extract_explanation* can be, extracting the top-K explanation based on the weights of the mask [52], or employing a pre-defined threshold [42].

Algorithm 1 The NSEG algorithm

Input: The trained GNN model f_θ , the instance to be explained $\mathcal{I} : \hat{y} = f_\theta(E_i, X_i)$, the hyper-parameters $(\alpha_e, \beta_e, \alpha_f, \beta_f)$, and the # epochs n .

Output: The explanation (E'_i, X'_i) .

Randomly initialize the M_e and M_f

for $j = 1, 2, \dots, n$ **do**

$\text{PNS}_{\text{lb}} \leftarrow$ the lower bound of PNS calculated by M_e and M_f with Eq.(19)

$\mathcal{L} \leftarrow$ the overall loss calculated with Eq. (20)

$M_e \leftarrow$ the edge mask updated by $\frac{\partial \mathcal{L}}{\partial M_e}$

$M_f \leftarrow$ the node feature mask updated by $\frac{\partial \mathcal{L}}{\partial M_f}$

end for

$(E'_i, X'_i) \leftarrow \text{extract_explanation}(M_e, M_f)$

5. NSEG Variants: Optimizing Only PN or PS

In this section, we present two variants of NSEG(PNS): NSEG(PN) and NSEG(PS). NSEG(PN) focuses on optimizing the Probability of Necessity (PN), considering only the necessity of the explanation. On the other hand, NSEG(PS) concentrates on optimizing the Probability of Sufficiency (PS), considering only the sufficiency of the explanation. These two variants are utilized in our ablation study.

5.1. PN and PS

In the NSEG variants, NSEG(PN) and NSEG(PS), our goal is to generate the most necessary explanation via NSEG(PN) and the most sufficient explanation via NSEG(PS). Theoretically, the probability of necessity, PN, and the probability of sufficiency, PS, which can quantify the necessity and sufficiency of explanation (ξ) to the model outcome \hat{y} respectively [32], are defined in Definition 4 and 5.

Definition 4. (*Probability of necessity of the explanation*).

$$PN(\xi) = P(\mathbf{Y}_{\xi^c} \neq \hat{y} | \xi, \mathbf{Y} = \hat{y}). \quad (21)$$

Definition 5. (*Probability of sufficiency of the explanation*).

$$PS(\xi) = P(\mathbf{Y}_\xi = \hat{y} | \xi^c, \mathbf{Y} \neq \hat{y}). \quad (22)$$

PN captures the probability that the model outcome \hat{y} changes with the absence of the event ξ , given the fact that the event ξ happens and the model outcome is \hat{y} . In similar, PS captures the probability that the model outcome is \hat{y} with the existence of the event ξ , given the fact that the event ξ does not happen, and the model outcome is not \hat{y} .

Similar to the generalized formulation in Eq. (4), both PN and PS in Eqs. (21) and (22) can be generalized to GNN explanation formulations, which are given as follows.

$$\begin{aligned} & \text{PN}^{e,f}(E'_i, X'_i) \\ &= P_\theta(\mathbf{Y}_{(\mathbf{E}=E'_i, \mathbf{X}=X'_i)^c} \neq \hat{y} | \mathbf{E} = E'_i, \mathbf{X} = X'_i, \mathbf{Y} = \hat{y}), \end{aligned} \quad (23)$$

$$\begin{aligned} & \text{PS}^{e,f}(E'_i, X'_i) \\ &= P_\theta(\mathbf{Y}_{\mathbf{E}=E'_i, \mathbf{X}=X'_i} = \hat{y} | (\mathbf{E} = E'_i, \mathbf{X} = X'_i)^c, \mathbf{Y} \neq \hat{y}), \end{aligned} \quad (24)$$

For NSEG(PN), to generate the most necessary explanation of GNN, the objective to maximize the PN defined in Eq. (23):

$$\max_{E'_i, X'_i} \text{PN}^{e,f}(E'_i, X'_i). \quad (25)$$

Similar for NSEG(PS), to generate the most sufficient explanation, the objective to maximize the PS defined in Eq. (24):

$$\max_{E'_i, X'_i} \text{PS}^{e,f}(E'_i, X'_i). \quad (26)$$

5.2. Optimization of PN and PS

The both PN and PS in Eqs. (23) and (24) are formulated as the probability of counterfactual in the literature of [33]. The identification of both PN and PS requires incorporating with SCM for the recovery of the exogenous [33]. However, the deterministic nature of GNN renders the given condition in the formulation of PN and PS not guaranteed, resulting in the non-identifiability of these probabilities. To better incorporate with the probability outputted by GNN, we derive lower bounds of both PN and PS that can be optimized in a similar fashion to PNS.

Proposition 3. *Given the SCM M depicted in Proposition 2, the lower bounds of $\text{PN}^{e,f}$ and $\text{PS}^{e,f}$ can be derived as:*

$$\begin{aligned} \text{PN}_{lb}^{e,f}(E'_i, X'_i) &= P_\theta(\mathbf{Y} \neq \hat{y} | (\mathbf{E} = E'_i, \mathbf{X} = X'_i)^c), \\ \text{PS}_{lb}^{e,f}(E'_i, X'_i) &= P_\theta(\mathbf{Y} = \hat{y} | \mathbf{E} = E'_i, \mathbf{X} = X'_i). \end{aligned}$$

The proof of Proposition 3 is given in Appendix A.5. Under the SCM M depicted in Proposition 2, the final optimizable formulations of $\text{PN}_{lb}^{e,f}$ and $\text{PS}_{lb}^{e,f}$ via continuous mask and sampling strategy are given as follows.

$$\begin{aligned} \text{PN}_{lb}^{e,f} &= 1 - P_{00} \mathbb{E}_{\epsilon_e, \epsilon_f} [f_\theta^{\hat{y}}((1 - M_e + \epsilon_e) \odot E_i, (1 - M_f + \epsilon_f) \odot X_i)] \\ &\quad - P_{01} \mathbb{E}_{\epsilon_e} [f_\theta^{\hat{y}}((1 - M_e + \epsilon_e) \odot E_i, M_f \odot X_i)] \\ &\quad - P_{10} \mathbb{E}_{\epsilon_f} [f_\theta^{\hat{y}}(M_e \odot E_i, (1 - M_f + \epsilon_f) \odot X_i)], \end{aligned} \quad (27)$$

$$\text{PS}_{ib}^{e,f} = f_{\theta}^y(M_e \odot E_i, M_f \odot X_i). \quad (28)$$

6. Empirical Study

In this section, we quantitatively and qualitatively evaluate our approach, NESG(PNS), on both synthetic and real-world data to tell if (1) the explanations are necessary and sufficient, and (2) the necessary and sufficient explanations are accurate. General information about the datasets and the experimental setups can be found in the following subsections, with more detailed information provided in Appendix B.

6.1. Dataset

In this subsection, we will introduce the datasets we used in our experiments, and the statistics of the dataset are presented in Table 1.

Table 1: Dataset statistics.

	BA-Shapes	Tree-Cycles	Tree-Grid	Mutagenicity	MSRC_21
# of graphs	1	1	1	4337	563
# of avg. nodes	700	871	1231	30.32	77.52
# of avg. edges	2055	967	1705	30.77	198.32
# of classes	4	2	2	2	20
feature type	-	-	-	one-hot	one-hot

Synthetic Datasets. We follow the graph generation process in an earlier study [52] and adopt three datasets for *node classification*, namely, BA-Shapes, Tree-Cycles, and Tree-Grid. Each dataset consists of a base graph and a set of motifs, where the class label of each node is determined by its role in the motif. For instance, in BA-Shapes, the motifs are the “house-shaped” subgraphs, and the class labels of the nodes are “bottom”, “middle”, “top” and “outside”. For a node instance, its ground-truth explanation is given by all edges in the motif to which it belongs.

Real-world Datasets. Two real-world datasets called Mutagenicity and MSRC_21 [31] are used for *graph classification* in our experiment. Mutagenicity contains chemical compounds that belong to two classes: either mutagenic or not. Each compound is a graph, in which each node is an atom and node features are one-hot encodings of the node atom types. In [27, 52, 42, 28], the amino-group (-NH2) and nitro-group (-NO2) are treated as the ground-truth explanations for the mutagenic compounds. Nevertheless, treating the sub-structure amino-group (-NH2) and nitro-group (-NO2) as ground-truth explanations is not rigorous, as it has been reported that among the compounds with aromatic -NO2 and -NH2 groups, only 76 % and 53 % of them are mutagenic [54]. Thus, we will not evaluate the explanation with accuracy metrics on Mutagenicity dataset. MSRC_21 is derived from MSRC-v2 [29], a benchmark dataset in semantic image processing, where each image belongs to one of the 20 classes describing the

scene of the image. A graph is constructed based on the semantic segmentation of each image, in which each node is a super-pixel whose feature is the one-hot embedding of the object semantic type.

6.2. Experimental Setup

GNN Training Setup. For both node and graph classification tasks, we employ three layers of Graph Convolutional Networks (GCNs) [20] with ReLU activations. For node classification task, we apply node-level read-out by stacking a fully connected classification layer after the last GCN layer. For graph classification task, a sum-based read-out is used to obtain a graph representation after the last GCN layer, followed by a fully connected classification layer. The detailed training setup and results are provided in Appendix B.1.

Evaluation Metrics. We utilize *Fidelity+* and *Fidelity-* (abbreviated as *Fid+* and *Fid-*) to quantify the necessity and sufficiency of the explanations, respectively. The higher *Fid+*, the more necessary the explanation, on the contrary, the lower *Fid-*, the more sufficient the explanation. Additionally, we use the *charact* score, which combines both *Fid+* and *Fid-*, to measure the overall performance on both necessary and sufficient aspects [2]. The definitions of *Fid+*, *Fid-* and *charact* scores are shown as follows.

$$\begin{aligned} Fid+ &= 1 - \frac{1}{N} \sum_{i=1}^N \mathbb{I}(\mathbf{Y}^{1-M} = \hat{y}), \\ Fid- &= 1 - \frac{1}{N} \sum_{i=1}^N \mathbb{I}(\mathbf{Y}^M = \hat{y}), \\ charact &= \frac{2 \times Fid+ \times (1 - Fid-)}{Fid+ + (1 - Fid-)}, \end{aligned}$$

where M is the explanation mask, and $\mathbf{Y}^{1-M} = f_{\theta}(E \odot (1 - M_e), X \odot (1 - M_f) + X^{cf} \odot M_f)$, and $\mathbf{Y}^M = f_{\theta}(E \odot M_e, X \odot M_f + X^{cf} \odot (1 - M_f))$. We use $Fid+^c$, $Fid-^c$ and $charact^c$ to denote these scores for continuous mask explanations. Since the discrete nature of graph, we further discretize the explanations mask via threshold (0.5), and compute the $Fid+^d$, $Fid-^d$ and $charact^d$ for discrete mask explanations.

Further, we use Top-K *Accuracy* and *ROC-AUC* to evaluate if the necessary and sufficient explanations are accurate. In particular, K equals the number of edges in the ground-truth explanation on synthetic datasets, i.e., 6/6/12 for BA-Shapes/Tree-Cycles/Tree-Grid. Besides, for Top-K *Accuracy* using nodes (e.g., PGM-Explainer), K equals 5/6/9 for BA-Shapes/Tree-Cycles/Tree-Grid.

Hyper-parameter Setting. The detailed hyper-parameters settings of NSEG(PNS^e) and NSEG(PNS^{e,f}) are shown in Table 2. Specifically, the hyper-parameters with sub-script (e) in 2 are used for M_e , while the hyper-parameters with sub-script (f) are used for M_f .

Table 2: The hyper-parameters setting of NSEG(PNS^e) and NSEG(PNS^{e,f}) among experimented datasets.

	BA-Shapes	Tree-Cycles	Tree-Grid	Mutagenicity	MSRC.21
PNS ^e					
α_e	5.0e-3	1.0e-2	1.0e-2	1.0e-4	1.0e-3
β_e	1.0	1.0	1.0	1.0e-3	1.0
PNS ^{e,f}					
α_e	5.0e-3	1.0e-2	1.0e-2	1.0e-4	5.0e-4
β_e	1.0	1.0	1.0	1.0e-3	1.0
α_f	5.0e-3	1.0e-3	1.0e-2	1.0e-4	5.0e-4
β_f	1.0	1.0	1.0	1.0e-3	1.0

Baselines. To verify the effectiveness of PNS, we consider three variants of NSEG, named NSEG(PN), NSEG(PS), and NSEG(PNS), which optimize the lower bound of the probability of necessity, the probability of sufficiency, and the probability of necessity and sufficiency respectively. Furthermore, we use a superscript to indicate if edge (e) or feature (f) is considered in the explanations, e.g., NSEG(PNS^e) means only edge explanations are considered by our full PNS model.

Our method is compared with the state-of-the-art baselines that generate perturbation-based explanations, including the following:

- **GNNEExplainer** [52] generates explanations by maximizing the mutual information between explanation subgraph and model prediction.
- **PGExplainer** [27] generates explanations from parameterized networks whose objective is to maximize the mutual information, similar to GNNEExplainer.
- **PGM-Explainer** [45] generates Bayesian networks as explanations upon the perturbation-prediction data to identify significant nodes. (Note that in the original implementation of PGM-Explainer, only nodes in the Bayesian networks are used for evaluation, thus in our experiment we only report the top-K *accuracy* using nodes instead of edges, and we will not report the *fidelity* since there is no edge explanation obtained.)
- **CF-GNNEExplainer** [25] generates counterfactual explanations capable of flipping the model prediction subject to minimal perturbation.
- **CF²** [42] generates explanations based on factual and counterfactual reasoning.

Regarding the implementations of baselines, we adopt their original settings, as detailed in Appendix B.2. Since all baseline approaches generate only edge explanations instead of the joint explanations of edge and node features, for a fair comparison, we mainly compare the results of NSEG(PNS^e), NSEG(PN^e), and NSEG(PS^e) (which only generate edge explanations) with baseline methods in quantitative analysis, and we also showcase the results of NSEG(PNS^{e,f}), which generate joint explanations, in both quantitative and qualitative analyses.

Table 3: Comparison of $Fid+^c$ (%), $Fid-^c$ (%) and $charact^c$ (%) of the explanations obtained by different approaches and variants of NSEG. Mean and 95 % confidence interval are reported. The best result of each metric is bolded.

	Node Classification									Graph Classification					
	BA-Shapes			Tree-Cycles			Tree-Grid			Mutagenicity			MSRC_21		
	$Fid+^c$ (%)	$Fid-^c$ (%)	$charact^c$ (%)	$Fid+^c$ (%)	$Fid-^c$ (%)	$charact^c$ (%)	$Fid+^c$ (%)	$Fid-^c$ (%)	$charact^c$ (%)	$Fid+^c$ (%)	$Fid-^c$ (%)	$charact^c$ (%)	$Fid+^c$ (%)	$Fid-^c$ (%)	$charact^c$ (%)
GNExplainer	46.95 ± 0.81	22.00 ± 0.00	35.08 ± 0.21	67.28 ± 1.21	20.89 ± 0.32	72.71 ± 0.84	30.03 ± 0.88	40.38 ± 0.83	71.58 ± 0.67	12.90 ± 1.51	80.44 ± 1.30	11.82 ± 1.21	85.56 ± 0.53	2.40 ± 0.00	92.20 ± 0.30
PGExplainer	58.45 ± 0.88	59.45 ± 0.10	47.88 ± 0.26	93.61 ± 4.30	95.56 ± 1.41	8.40 ± 2.57	88.06 ± 10.86	94.63 ± 1.51	10.10 ± 2.71	95.20 ± 0.00	95.20 ± 0.00	9.14 ± 0.00	80.64 ± 1.75	80.96 ± 1.96	30.77 ± 2.66
CF-GNNEExplainer	33.85 ± 0.32	79.75 ± 0.00	25.34 ± 0.07	78.39 ± 0.61	6.11 ± 0.00	85.44 ± 0.36	43.78 ± 0.41	59.55 ± 0.65	42.05 ± 0.49	93.76 ± 1.02	95.20 ± 0.00	9.13 ± 0.00	70.16 ± 1.46	91.60 ± 0.00	15.13 ± 0.03
CF	46.60 ± 0.25	72.00 ± 0.00	34.68 ± 0.07	78.39 ± 0.00	21.11 ± 0.00	78.89 ± 0.00	43.89 ± 0.00	56.11 ± 0.00	43.89 ± 0.00	98.88 ± 0.16	9.80 ± 0.00	90.94 ± 0.08	97.20 ± 0.00	92.24 ± 0.19	64.63 ± 0.17
NSEG(PN ^e)	100.00 ± 0.00	72.25 ± 0.00	43.44 ± 0.00	100.00 ± 0.00	0.00 ± 0.00	100.00 ± 0.00	59.86 ± 0.00	13.58 ± 0.13	92.65 ± 0.08	99.90 ± 0.20	83.30 ± 0.20	28.62 ± 0.29	96.40 ± 0.00	51.70 ± 0.20	64.36 ± 0.17
NSEG(PN ^s)	92.75 ± 0.00	6.00 ± 0.00	77.11 ± 0.00	98.39 ± 0.01	0.00 ± 0.00	59.41 ± 0.01	57.63 ± 0.00	0.00 ± 0.00	98.81 ± 0.00	91.33 ± 0.09	0.27 ± 0.20	95.35 ± 0.30	43.60 ± 0.45	35.87 ± 0.26	43.86 ± 0.35
NSEG(PN ^s) ^e	97.90 ± 0.12	6.00 ± 0.00	88.94 ± 0.06	100.00 ± 0.00	0.00 ± 0.00	100.00 ± 0.00	100.00 ± 0.00	0.00 ± 0.00	100.00 ± 0.00	59.60 ± 0.00	0.80 ± 0.00	99.40 ± 0.00	96.00 ± 0.00	33.12 ± 0.46	78.84 ± 0.32
NSEG(PN ^s) ^e ^f	100.00 ± 0.00	0.00 ± 0.00	100.00 ± 0.00	100.00 ± 0.00	0.00 ± 0.00	100.00 ± 0.00	100.00 ± 0.00	0.00 ± 0.00	100.00 ± 0.00	95.20 ± 0.00	44.08 ± 1.25	70.45 ± 0.99	93.52 ± 0.38	61.44 ± 0.19	54.61 ± 0.24

Table 4: Comparison of $Fid+^d$ (%), $Fid-^d$ (%) and $charact^d$ (%) of the explanations obtained by different approaches and variants of NSEG. Mean and 95 % confidence interval are reported. The best result of each metric is bolded.

	Node Classification									Graph Classification					
	BA-Shapes			Tree-Cycles			Tree-Grid			Mutagenicity			MSRC_21		
	$Fid+^d$ (%)	$Fid-^d$ (%)	$charact^d$ (%)	$Fid+^d$ (%)	$Fid-^d$ (%)	$charact^d$ (%)	$Fid+^d$ (%)	$Fid-^d$ (%)	$charact^d$ (%)	$Fid+^d$ (%)	$Fid-^d$ (%)	$charact^d$ (%)	$Fid+^d$ (%)	$Fid-^d$ (%)	$charact^d$ (%)
GNExplainer	95.40 ± 0.25	72.00 ± 0.00	43.29 ± 0.03	51.06 ± 1.42	20.39 ± 0.28	62.20 ± 1.06	92.44 ± 0.68	38.36 ± 0.70	73.96 ± 0.56	110.08 ± 1.69	89.76 ± 1.01	10.11 ± 1.22	88.40 ± 0.25	2.72 ± 0.16	92.63 ± 0.15
PGExplainer	89.55 ± 4.80	71.00 ± 0.57	40.28 ± 14.09	13.96 ± 0.11	10.90 ± 0.34	29.53 ± 12.42	95.42 ± 0.00	50.02 ± 0.14	90.21 ± 0.13	95.20 ± 0.00	3.20 ± 0.00	95.99 ± 0.00	15.60 ± 14.41	85.70 ± 7.98	13.61 ± 11.90
CF-GNNEExplainer	92.00 ± 0.00	79.75 ± 0.00	33.19 ± 0.00	30.50 ± 1.33	6.11 ± 0.00	46.03 ± 1.51	55.42 ± 0.38	77.78 ± 0.63	31.72 ± 0.66	3.04 ± 0.59	95.20 ± 0.00	3.69 ± 0.46	32.48 ± 1.27	92.08 ± 0.29	12.72 ± 0.32
CF	99.25 ± 0.00	72.00 ± 0.00	43.68 ± 0.00	28.67 ± 0.47	14.28 ± 0.47	42.96 ± 0.53	55.17 ± 0.23	56.33 ± 0.07	48.75 ± 0.06	96.56 ± 0.19	0.80 ± 0.00	97.86 ± 0.10	97.04 ± 0.19	51.20 ± 0.00	64.23 ± 0.04
NSEG(PN ^e)	79.75 ± 0.00	67.83 ± 0.16	69.87 ± 0.08	49.50 ± 0.32	6.11 ± 0.00	64.82 ± 0.27	59.28 ± 0.53	34.64 ± 0.75	62.17 ± 0.62	75.30 ± 0.49	79.20 ± 0.96	32.59 ± 1.16	96.40 ± 0.00	51.70 ± 0.20	64.36 ± 0.17
NSEG(PN ^s)	58.50 ± 0.15	1.20 ± 0.18	73.49 ± 0.17	18.72 ± 0.59	4.00 ± 0.28	31.33 ± 0.82	97.22 ± 0.00	0.00 ± 0.00	98.59 ± 0.00	75.07 ± 2.04	0.67 ± 0.26	85.50 ± 1.33	43.60 ± 0.45	54.87 ± 0.26	43.86 ± 0.35
NSEG(PN ^s) ^e	77.49 ± 0.12	0.85 ± 0.12	86.94 ± 0.06	23.83 ± 0.56	5.83 ± 0.00	20.30 ± 0.70	99.14 ± 0.10	0.00 ± 0.00	99.57 ± 0.05	97.92 ± 0.29	0.80 ± 0.00	98.56 ± 0.15	96.00 ± 0.00	33.12 ± 0.46	78.84 ± 0.32
NSEG(PN ^s) ^e ^f	79.75 ± 0.00	2.00 ± 0.00	87.94 ± 0.00	21.61 ± 0.11	5.83 ± 0.00	35.15 ± 0.14	73.53 ± 0.14	0.00 ± 0.00	84.74 ± 0.09	84.32 ± 0.63	42.48 ± 1.30	68.38 ± 0.87	93.52 ± 0.38	61.44 ± 0.19	54.61 ± 0.24

6.3. Are the Explanations Necessary and Sufficient?

We evaluate the necessity and sufficiency aspects of the explanations based on the $Fid+$, $Fid-$, and $charact$ metrics [2] in Table 3 and Table 4 for continuous and discrete explanations, respectively.

Firstly, when comparing with the baselines, NSEG(PN^s) (including NSEG(PN^s^e) and NSEG(PN^s^{e,f})) consistently outperforms the other methods, achieving the highest $charact^c$ scores for continuous explanations in most cases and the second winner on MSRC_21 dataset. When discrete explanations are obtained by thresholding, NSEG(PN^s) achieves the best $charact^d$ scores in most cases and the second best on MSRC_21. The second best results on MSRC_21 can be due to, the winner GNExplainer that searches for sufficient explanations yields the extremely lowest $Fid-^c$ and $Fid-^d$, thus leads to the highest $charact^c$ and $charact^d$, respectively.

Secondly, among the variants of NSEG, we observe that NSEG(PN^e) provides higher $Fid+^c$ and $Fid+^d$ scores compared to NSEG(PN^s), indicating that NSEG(PN^e) focuses more on necessity. Conversely, NSEG(PN^s) emphasizes sufficiency, as reflected by its lower $Fid-^c$ and $Fid-^d$ scores compared to NSEG(PN^e). The full model, NSEG(PN^s^e), combines the benefits of both aspects, achieving the highest $charact^c$ and $charact^d$ scores in most cases, with one exception on $charact^d$ on Tree-Cycles datasets. This can be due to, the discretization process damages the necessary aspect of the explanation leading to extremely low $Fid+^d$, thus causes low $charact^d$.

In summary, NSEG(PN^s) consistently generates the most necessary and sufficient explanations in most cases compared to the baselines and other variants of our approach.

6.4. Are the Necessary and Sufficient Explanations Accurate?

We employ top-K *accuracy* (Acc) and *ROC-AUC* (AUC) to judge if the necessary and sufficient explanations are accurate. As there is only edge-based

Table 5: Comparison of Top-K *Accuracy* (%) and *ROC-AUC* (%) of the explanations obtained by different approaches. Mean and 95 % confidence interval are reported. The best result of each metric is bolded.

	BA-Shapes		Tree-Cycles		Tree-Grid	
	Acc (Top-K)	AUC	Acc (Top-K)	AUC	Acc (Top-K)	AUC
GNNExplainer	71.77 ± 0.67	85.09 ± 0.30	62.48 ± 0.23	50.89 ± 0.42	71.06 ± 0.14	57.34 ± 0.30
PGExplainer	83.67 ± 11.26	95.19 ± 3.22	83.29 ± 8.81	81.97 ± 8.86	61.19 ± 1.91	53.91 ± 3.43
PGM-Explainer	65.01 ± 0.69	-	82.35 ± 0.69	-	72.91 ± 0.20	-
CF-GNNExplainer	74.33 ± 0.15	81.24 ± 0.11	77.01 ± 0.15	63.49 ± 0.15	74.75 ± 0.11	66.74 ± 0.07
CF ²	80.31 ± 0.22	89.77 ± 0.06	71.57 ± 0.49	60.21 ± 0.34	69.67 ± 0.09	61.18 ± 0.09
NSEG(PNS ^e)	88.55 ± 0.05	96.57 ± 0.01	80.18 ± 0.26	65.73 ± 0.15	75.36 ± 0.05	66.46 ± 0.08
NSEG(PNS ^{e,f})	90.02 ± 0.09	98.10 ± 0.06	69.33 ± 0.08	66.76 ± 0.10	75.44 ± 0.03	66.87 ± 0.09

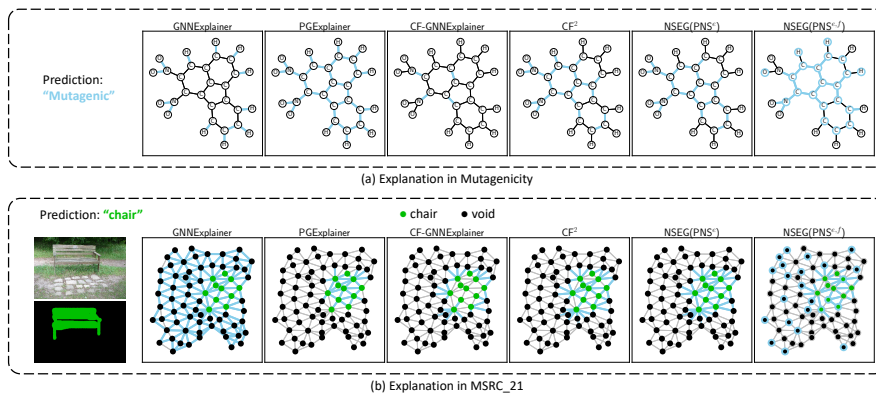


Figure 4: Explanations of GNNExplainer, PGExplainer, CF-GNNExplainer, CF², NSEG(PNS^e), and NSEG(PNS^{e,f}) in Mutagenicity and MSRC_21, where the explanations are highlighted in blue.

ground truth on the first three synthetic datasets, we only generate edge explanations using NSEG(PNS^e) on those datasets compared with the other baselines, as shown in Table 5.

The results indicate that our approach generally achieves the highest accuracy except on Tree-Cycles datasets. The slightly lower top-K *accuracy* and *ROC-AUC* of our approach on Tree-Cycles may be attributed to the fact that NSEG prioritizes finding the most necessary and sufficient explanations rather than focusing on ranking the explanations. However, top-K *accuracy* and *ROC-AUC* metrics are sensitive to ranking, which could explain the relative difference in performance on Tree-Cycles.

6.5. Qualitative Studies

Besides quantitative analysis, visual explanations can better help humans understand the decision-making process of GNNs. Hence, we present a series of qualitative studies as follows.

Explanations of NSEG and Baselines. Figure 4 illustrates explanations obtained by different approaches in Mutagenicity and MSRC_21 datasets. In Figure 4 (a), we observe that NSEG(PNS) successfully identifies the well-known

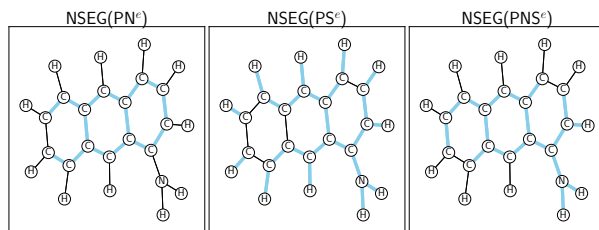


Figure 5: Explanations of NSEG variants, NSEG(PN^e), NSEG(PS^e), and NSEG(PNS^e) on a Mutagenicity instance, where the explanations are highlighted in blue.

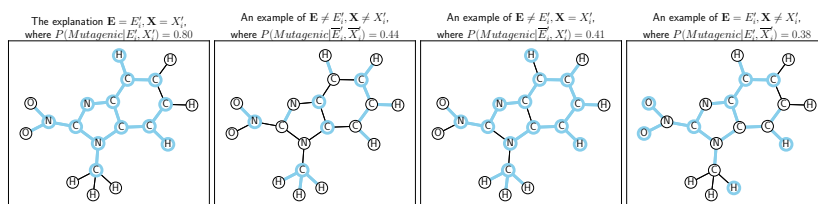
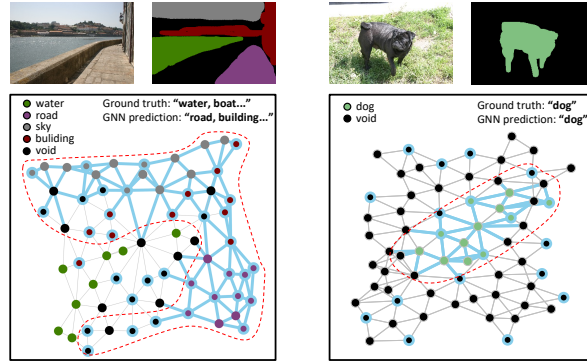


Figure 6: Explanation of NSEG(PNS^{e,f}) on a Mutagenicity instance, where the explanation is highlighted in blue.

explanation, the nitro-group (-NO₂), in the Mutagenicity dataset, while maintaining the integrity of the molecule by including the benzene ring and excluding the hydrogen bond (-H). Additionally, NSEG(PNS^{e,f}) generates a finer-grained explanation by identifying the node features of nitrogen (N), oxygen (O), and carbon (C) atoms. In Figure 4 (b), the prediction of the instance graph is a scene about “chair”. We observe that our approach NSEG(PNS) successfully identifies all edges among the node “chair” as the explanation, while GNNExplainer generates the explanation including not only edges among nodes “chair” but also edges among nodes “void”, and CF-GNNExplainer only identifies the edges between nodes “chair” and nodes “void”.

Explanations of NSEG Variants. Figure 5 illustrates the explanations obtained by the variants of NSEG, which are NSEG(PN^e), NSEG(PS^e), and NSEG(PNS^e) respectively. Compared to the baselines, NSEG(PNS^e) identifies the well-known explanation, the amino-group (-NH₂) [52, 27], while keeping the integrity of the molecule by including the benzene ring and excluding the hydrogen bond (-H). In contrast, the ablation NSEG(PN^e) only identifies the benzene ring (which is necessary but not sufficient), while NSEG(PS^e) identifies almost the whole graph (which is sufficient but not necessary).

Explanations with both Necessity and Sufficiency. In Figure 6 a compound is predicted as a “mutagenic”, whose necessary and sufficient explanation $\mathbf{E} = E_i'$, $\mathbf{X} = X_i'$ can produce the prediction “mutagen” with a high probability 0.93, showing the sufficiency of the explanation. Also, in the last three columns of Figure 6, we present one example for each of the cases: $(\mathbf{E} \neq E_i', \mathbf{X} \neq X_i')$,



(a) Explanation of an incorrectly predicted instance. The GNN falsely pays more attention to the nodes “sky”, “road”, and “building” and the edges among them.

(b) Explanation of a correctly predicted instance. The GNN correctly pays more attention to the nodes “dog” and the edges among them.

Figure 7: Explanations of $\text{NSEG}(\text{PNS}^{e,f})$ on two MSRC_21 instances, where the explanations are highlighted in blue and enclosed by a red dashed line.

($\mathbf{E} \neq E'_i, \mathbf{X} = X'_i$), and ($\mathbf{E} = E'_i, \mathbf{X} \neq X'_i$), which degrades the probabilities of producing “mutagen” to 0.44, 0.41, and 0.38, respectively. Such changes imply the necessity of the explanation.

Explanations for Incorrect and Correct Predictions. To gain insights into the model’s decision-making process, it is crucial to explain both correct and incorrect predictions. Hence, we showcase two explanations of the instances with correct and incorrect predictions. The first instance in Figure 7(a) is a scene about “water, boat...”, but the GNN incorrectly predicts “road, building...”. The generated explanation suggests the reason behind the misclassification—the GNN paid more attention to the nodes “road”, “building”, and the edges among them. The second instance in Figure 7(b) is a scene about “dog”, which is correctly predicted. The generated explanation shows that more attention was paid to the nodes “dog” and edges among them, leading to the correct prediction.

Additionally, more qualitative studies are shown in Appendix C.

7. Conclusion

In this paper, we proposed NSEG, a GNN explanation model that is able to provide necessary and sufficient explanations for GNNs. Different from the existing approaches that generate either necessary or sufficient explanations, or a heuristic trade-off explanation between the two aspects, our objective is to maximize PNS that ensures the explanation is both necessary and sufficient. To overcome the intractability of identifying PNS, we derived a lower bound

of PNS, and further propose a generalized SCM of GNN for estimating this lower bound. For optimization, we leverage continuous masks with sampling strategy to optimize the lower bound. Our empirical study demonstrates that NSEG can provide the most necessary and sufficient explanations and achieves state-of-the-art performance on various datasets.

Appendix A. Proof

Appendix A.1. Proof of Lemma 1

Proof. According to the definition of PNS in Definition 2, we have

$$\begin{aligned} & \text{PNS}(\xi) \\ &= P(\mathbf{Y}_{\xi^c} \neq \hat{y}, \mathbf{Y}_{\xi} = \hat{y}) \\ &= P(\mathbf{Y}_{\xi^c} \neq \hat{y}) + P(\mathbf{Y}_{\xi} = \hat{y}) - P(\mathbf{Y}_{\xi^c} \neq \hat{y} \vee \mathbf{Y}_{\xi} = \hat{y}), \end{aligned}$$

since $P(\mathbf{Y}_{\xi^c} \neq \hat{y} \vee \mathbf{Y}_{\xi} = \hat{y}) \leq 1$ and $P(\mathbf{Y}_{\xi^c} \neq \hat{y}, \mathbf{Y}_{\xi} = \hat{y}) \geq 0$, we have:

$$\text{PNS}(\xi) \geq \max\{0, P(\mathbf{Y}_{\xi^c} \neq \hat{y}) + P(\mathbf{Y}_{\xi} = \hat{y}) - 1\}.$$

□

Appendix A.2. Proof of Lemma 2

Proof. Since $(\mathbf{Y}_{\xi^c} = \hat{y}) \vee (\mathbf{Y}_{\xi^c} \neq \hat{y}) = \text{true}$, we have:

$$\begin{aligned} & (\mathbf{Y}_{\xi} = \hat{y}) \\ &= (\mathbf{Y}_{\xi} = \hat{y}) \wedge ((\mathbf{Y}_{\xi^c} = \hat{y}) \vee (\mathbf{Y}_{\xi^c} \neq \hat{y})) \\ &= ((\mathbf{Y}_{\xi} = \hat{y}) \wedge (\mathbf{Y}_{\xi^c} = \hat{y})) \vee ((\mathbf{Y}_{\xi} = \hat{y}) \wedge (\mathbf{Y}_{\xi^c} \neq \hat{y})), \end{aligned}$$

and since $(\mathbf{Y}_{\xi} = \hat{y}) \vee (\mathbf{Y}_{\xi} \neq \hat{y}) = \text{true}$, when monotonicity holds, i.e., $(\mathbf{Y}_{\xi} \neq \hat{y}) \wedge (\mathbf{Y}_{\xi^c} = \hat{y}) = \text{false}$, we have:

$$\begin{aligned} & (\mathbf{Y}_{\xi^c} = \hat{y}) \\ &= (\mathbf{Y}_{\xi^c} = \hat{y}) \wedge ((\mathbf{Y}_{\xi} = \hat{y}) \vee (\mathbf{Y}_{\xi} \neq \hat{y})) \\ &= ((\mathbf{Y}_{\xi^c} = \hat{y}) \wedge (\mathbf{Y}_{\xi} = \hat{y})) \vee ((\mathbf{Y}_{\xi^c} = \hat{y}) \wedge (\mathbf{Y}_{\xi} \neq \hat{y})) \\ &= ((\mathbf{Y}_{\xi^c} = \hat{y}) \wedge (\mathbf{Y}_{\xi} \neq \hat{y})), \end{aligned}$$

then, combining those 2 equations, we have:

$$\begin{aligned} & (\mathbf{Y}_{\xi} = \hat{y}) \\ &= (\mathbf{Y}_{\xi^c} = \hat{y}) \vee ((\mathbf{Y}_{\xi} = \hat{y}) \wedge (\mathbf{Y}_{\xi^c} \neq \hat{y})) \end{aligned}$$

then take the probability form and use the disjointness of $\mathbf{Y}_{\xi^c} = \hat{y}$ and $\mathbf{Y}_{\xi^c} \neq \hat{y}$:

$$\begin{aligned} & P(\mathbf{Y}_{\xi} = \hat{y}) \\ &= P(\mathbf{Y}_{\xi^c} = \hat{y}) + P(\mathbf{Y}_{\xi} = \hat{y}, \mathbf{Y}_{\xi^c} \neq \hat{y}) \end{aligned}$$

then:

$$\begin{aligned}
& \text{PNS}(\xi) \\
&= P(\mathbf{Y}_\xi = \hat{y}) - P(\mathbf{Y}_{\xi^c} = \hat{y}) \\
&= P(\mathbf{Y}_\xi = \hat{y}) + P(\mathbf{Y}_{\xi^c} \neq \hat{y}) - 1
\end{aligned}$$

□

Appendix A.3. Proof of Proposition 1

Proof. In a graph neural network, each node's hidden representation in each hidden layer can be written as functions of entries of graph and all nodes' representations in the previous layer, i.e.,

$$\forall v \forall k (\mathbf{h}_v^{(k)} = f_\theta^{(k)}(\mathbf{E}_{*,i}, \mathbf{H}^{(k-1)})),$$

where $\mathbf{h}_v^{(k)}$ denotes the hidden representation of node v in k -th layer, $\mathbf{H}^{(k-1)}$ denotes the hidden representations of all nodes in $(k-1)$ -th layer, $\mathbf{E}_{*,i}$ denotes the entries from all nodes to node i . Then for all nodes' representations, we have,

$$\forall k (\mathbf{H}^{(k)} = f_\theta^{(k)}(\mathbf{E}, \mathbf{H}^{(k-1)})),$$

where \mathbf{E} denotes the edges of the graph.

The output variable \mathbf{Y} is determined by all nodes' representations in l -th layer by a read-out function $f_\theta^{(l+1)}$ (specifically, a node-level read-out for node classification task and a graph-level read-out for graph classification task), i.e.,

$$\mathbf{Y} = f_\theta^{(l+1)}(\mathbf{H}^{(l)}).$$

And for the input variables \mathbf{E} and \mathbf{X} , they are determined by a set of exogenous \mathbf{U} , i.e.,

$$\mathbf{E}, \mathbf{X} = f^{(0)}(\mathbf{U}).$$

Thus, the structure of those variables can be equivalently expressed by a SCM $M(\{\mathbf{X}, \mathbf{E}, \mathbf{H}^{(1)}, \dots, \mathbf{H}^{(l)}, \mathbf{Y}\}, \mathbf{U}, \{f^{(0)}, f_\theta^{(1)}, \dots, f_\theta^{(l+1)}\})$. □

Appendix A.4. Proof of Proposition 2

Proof. Start from the output variable \mathbf{Y} , the corresponding causal mechanism function $\mathbf{Y} = f_\theta^{(l+1)}(\mathbf{H}^{(l)})$ can be substituted as

$$\mathbf{Y} = f_\theta^{(l+1)}(f_\theta^{(l)}(\mathbf{E}, f_\theta^{(l-1)}(\mathbf{E}, \dots f_\theta^{(1)}(\mathbf{E}, \mathbf{X}))).$$

Thus, we can obtain a new causal mechanism f_θ that is a mapping from \mathbf{E}, \mathbf{X} to \mathbf{Y} , i.e.,

$$\mathbf{Y} = f_\theta(\mathbf{E}, \mathbf{X}).$$

Hence, we can obtain a reduced SCM $M(\{\mathbf{E}, \mathbf{X}, \mathbf{Y}\}, \mathbf{U}, \{f^{(0)}, f_\theta\})$. □

Appendix A.5. Proof of Proposition 3

Proof. First, we can derive lower bounds of both PN and PS as follows.

$$\begin{aligned}
\text{PN}(\xi) &= P(\mathbf{Y}_{\xi^c} \neq \hat{y} | \xi, \mathbf{Y} = \hat{y}) \\
&= \frac{P(\mathbf{Y}_{\xi^c} \neq \hat{y}, \xi, \mathbf{Y} = \hat{y})}{P(\xi, \mathbf{Y} = \hat{y})} \\
&\geq \frac{\max\{0, P(\mathbf{Y}_{\xi^c} \neq \hat{y}) + P(\xi, \mathbf{Y} = \hat{y}) - 1\}}{P(\xi, \mathbf{Y} = \hat{y})} \\
&= \max\left\{0, \frac{P(\mathbf{Y}_{\xi^c} \neq \hat{y}) + P(\xi, \mathbf{Y} = \hat{y}) - 1}{P(\xi, \mathbf{Y} = \hat{y})}\right\} \\
&= \max\left\{0, 1 + \frac{P(\mathbf{Y}_{\xi^c} \neq \hat{y}) - 1}{P(\xi, \mathbf{Y} = \hat{y})}\right\} \\
&\geq \max\{0, P(\mathbf{Y}_{\xi^c} \neq \hat{y})\} = P(\mathbf{Y}_{\xi^c} \neq \hat{y}) \\
\text{PS}(\xi) &= P(\mathbf{Y}_\xi = \hat{y} | \xi^c, \mathbf{Y} \neq \hat{y}) \\
&= \frac{P(\mathbf{Y}_\xi = \hat{y}, \xi^c, \mathbf{Y} \neq \hat{y})}{P(\xi^c, \mathbf{Y} \neq \hat{y})} \\
&\geq \frac{\max\{0, P(\mathbf{Y}_\xi = \hat{y}) + P(\xi^c, \mathbf{Y} \neq \hat{y}) - 1\}}{P(\xi^c, \mathbf{Y} \neq \hat{y})} \\
&= \max\left\{0, \frac{P(\mathbf{Y}_\xi = \hat{y}) + P(\xi^c, \mathbf{Y} \neq \hat{y}) - 1}{P(\xi^c, \mathbf{Y} \neq \hat{y})}\right\} \\
&= \max\left\{0, 1 + \frac{P(\mathbf{Y}_\xi = \hat{y}) - 1}{P(\xi^c, \mathbf{Y} \neq \hat{y})}\right\} \\
&\geq \max\{0, P(\mathbf{Y}_\xi = \hat{y})\} = P(\mathbf{Y}_\xi = \hat{y})
\end{aligned}$$

Altering the event ξ with the explanation event ($\mathbf{E} = E'_i, \mathbf{X} = X'_i$), and under the SCM depict in Proposition 2, the lower bounds of PN and PS after intervening on both \mathbf{E} and \mathbf{X} (replacing causal mechanism from \mathbf{U} to \mathbf{E} and \mathbf{X}), we have:

$$\begin{aligned}
\text{PN}_{lb}^{e,f}(E'_i, X'_i) &= P_\theta(\mathbf{Y} \neq \hat{y} | (\mathbf{E} = E'_i, \mathbf{X} = X'_i)^c), \\
\text{PS}_{lb}^{e,f}(E'_i, X'_i) &= P_\theta(\mathbf{Y} = \hat{y} | \mathbf{E} = E'_i, \mathbf{X} = X'_i).
\end{aligned}$$

□

Appendix B. Details of Experiment Setup

Appendix B.1. GNN Training Setup

In this section, we introduce the training setup and training result of the GNN we explain. For the GNN training, we employ three layers of Graph Convolutional Networks (GCNs) [20] with ReLU activation. For node classification task, the dimensions of the hidden layers are 16, 32, and 16 respectively, followed by a fully connected layer as the output layer. For graph classification task, the

Table B.6: The hyperparameter setting and test accuracy of GNN.

	BA-Shapes	Tree-Cycles	Tree-Grid	Mutagenicity	MSRC.21
lr	0.001	0.001	0.001	0.001	0.001
# of GNN layers	3	3	3	3	3
# of epochs	2000	2000	2000	500	500
dropout	0	0	0	0.5	0.5
optimizer	Adam	Adam	Adam	Adam	Adam
weight decay	0	0	0	5e-4	5e-4
accuracy	0.957	0.903	0.927	0.761	0.983

dimensions of the hidden layer in graph classification task are 16, 32, and 16, and after the last GCN layer, a sum-based read-out is used to obtain a graph representation, followed by a fully connected layer as the output layer. For all datasets, we split train/test with 80 %/20 %. The hyperparameter setting and test accuracy of the trained GNN model are shown in Table B.6.

Appendix B.2. Baselines

GNNE explainer. The goal of GNNE explainer is to identify a subgraph G'_i and the associated features X'_i that are important to GNN’s prediction \hat{y} . The objective of GNNE explainer is to maximize the mutual information between the subgraph explanation and the GNN model outcome. Intuitively, if knowing the information of the subgraph G'_i and its associated features X'_i can reduce the uncertainty of \mathbf{Y} , then G'_i and X'_i are good explanations for the GNN prediction. Equivalently, the mutual information objective captures the sufficiency aspect in producing an explanation.

$$\max_{G'_i, X'_i} MI(\mathbf{Y}; (G'_i, X'_i))$$

where MI quantifies the change in the probability of the prediction \hat{y} when the input is limited to (G'_i, X'_i) . In particular, GNNE explainer converts the discrete optimization problem into continuous optimization and leverages trainable edge mask M_e and feature mask M_f in optimization, where the objective is derived as follow.

$$\min_{M_e, M_f} H(\mathbf{Y} | \mathbf{G} = G_i \odot M_e, \mathbf{X} = X_i \odot M_f)$$

Notably, the X'_i in GNNE explainer is quite different from the X'_i in NSEG, where the former is a feature dimension-wise explanation while the latter is a node-wise explanation. In implementations, we adopt the original settings where for node classification task the l -hop subgraph of the target node is extracted, where l denotes the number of graph convolution layers. For hyper-parameter that controls the *mask size* regularization, we select [0.01, 0.01, 0.01, 0.005, 0.005] for BA-Shapes, Tree-Cycles, Tree-Grid, Mutagenicity, and MSRC.21, respectively. For hyper-parameter that controls the *entropy* regularization, we set it to 1.0 for all datasets.

PGExplainer. Though PGExplainer shares the same objective with GNNExplainer, i.e., maximizing the mutual information between the subgraph explanation and the GNN outcome, PGExplainer spends way less time in inference than GNNExplainer. To achieve this, the key idea of PGExplainer is to learn a mapping from the graph representation space to subgraph space parameterized by ω , and the subgraphs are sampled from the distribution $q(\omega)$. The parameterized mapping gives PGExplainer the inductive ability, which means the explainer once trained, it does not need to be retrained to explain different instances. In particular, the objective of PGExplainer is shown as follows.

$$\min_{\omega} \mathbb{E}_{G'_i \sim q(\omega)} H(\mathbf{Y} | G'_i),$$

where the sampling process $G'_i \sim q(\omega)$ is approximated via determinant function of parameters ω , temperature τ , and an independent random variable $\epsilon \sim U(0, 1)$:

$$G'_i = f_{\omega}(G_i, \tau, \epsilon).$$

In implementations, we adopt the original annealing schedule of τ , i.e., $\tau_t = (\tau_T/\tau_0)^t$, where τ_0 and τ_T are set to 5.0 and 2.0, respectively. For node classification task the l -hop subgraph of the target node is extracted, where l denotes the number of graph convolution layers. For the hyper-parameter that controls the *mask size* regularization, we select [0.01, 0.01, 0.01, 0.05, 0.05] for BA-Shapes, Tree-Cycles, Tree-Grid, Mutagenicity, and MSRC_21, respectively. For the hyper-parameter that controls the *entropy* regularization, we set it to 1.0 for all datasets.

PGM-Explainer. A Probabilistic Graphical Model (PGM) is utilized as a surrogate in PGM-Explainer to generate explanations for GNN. The goal of PGM-Explainer is to learn a Bayesian network upon the local perturbation-prediction dataset to identify significant nodes. Specifically, to obtain the local perturbation-prediction dataset, PGM-Explainer randomly perturbs the node features of several random nodes, then records a random variable indicating whether its features are perturbed and its influence on the GNN predictions. After obtaining the local dataset, the Grow-Shrink (GS) algorithm is leveraged to reduce the size of the local dataset, then an interpretable Bayesian network is employed to fit the local dataset and to explain the GNN model. For hyper-parameters settings, we set the probability of perturbation to 0.5, the prediction difference threshold to 0.1, the number of samples to 50, and the p-value for the conditional independence test to 0.05.

CF-GNNExplainer. Different from GNNExplainer and PGExplainer whose objective is to generate subgraphs that are especially relevant for a particular prediction, the goal of CF-GNNExplainer is to generate a counterfactual explanation that can flip the model prediction. The nature of counterfactual explanation [25] is that the explanation can flip the model prediction subject to a minimal perturbation on data, which is equivalent to the nature of the necessary explanation. To generate the counterfactual explanation G'_i , the objective

of CF-GNNExplainer is given as follows.

$$\max_{G'_i} \mathcal{L}_{pred}(G_i, G'_i) + \beta \mathcal{L}_{dist}(G_i, G'_i),$$

where $\mathcal{L}_{pred}(G_i, G'_i)$ stands for the prediction loss aiming to obtain G'_i that can flip the model prediction, and $\mathcal{L}_{dist}(G_i, G'_i)$ stands for the distance loss aiming to achieve minimum perturbation. In implementations, we adopt the original settings where for node classification task the $(l+1)$ -hop subgraph of the target node is extracted, where l denotes the number of graph convolution layers. For β we select [0.05, 0.05, 0.05, 0.01, 0.01] for BA-Shapes, Tree-Cycles, Tree-Grid, Mutagenicity, and MSRC_21, respectively.

CF². *CF²* produces a trade-off explanation between necessity and sufficiency by taking insights into counterfactual and factual reasoning from causal inference theory. The objective of *CF²* is to minimize the complexity of the explanation, subject to the explanation strength being strong enough. The explanation strength can be divided into two parts, the counterfactual explanation strength S_c and the factual explanation strength S_f , and a hyperparameter is introduced to control the trade-off between the two. Formally, the objective of *CF²* is shown as follows.

$$\min_{G'_i, X'_i} C(G'_i) \quad s.t. \quad \alpha S_f(G'_i, X'_i) + (1 - \alpha) S_c(G'_i, X'_i) > \lambda,$$

where $C(G'_i, X'_i)$ measures the complexity of the explanation G'_i , and X'_i is similar to the X'_i of GNNExplainer as we mentioned before. For implementations, we adopt the original settings where α is set to 0.6 for all datasets, and λ is set to [500, 500, 500, 1000, 1000] for BA-Shapes, Tree-Cycles, Tree-Grid, Mutagenicity, and MSRC_21, respectively. Also for node classification task the l -hop subgraph of the target node is extracted, where l denotes the number of graph convolution layers.

Appendix B.3. Hardware and Software

For hardware, our experiments are conducted on on a Linux machine with Nvidia GeForce RTX 2080 Ti with 11 GB memory. For software, we implement our NSEG in Deep Graph Library (DGL) with Pytorch. For the implementations of the baseline approaches, we follow and modify the following codes: GNNExplainer (<https://github.com/RexYing/gnn-model-explainer>), PGExplainer (<https://github.com/flyingdoog/PGExplainer>), PGM-Explainer (https://github.com/mims-harvard/GraphXAI/tree/main/graphxai/explainers/pgm_explainer), CF-GNNExplainer (<https://github.com/a-lucic/cf-gnnexplainer>), and *CF²* (https://github.com/chrisjtan/gnn_cff).

Appendix C. More Qualitative Studies

We further illustrate the necessary and sufficient explanation obtained by our approach through visualization in more case studies. The visualization of explanations of Mutagenicity is shown in Figure C.8, while the visualization of explanations of MSRC_21 is shown in Figure C.9.

References

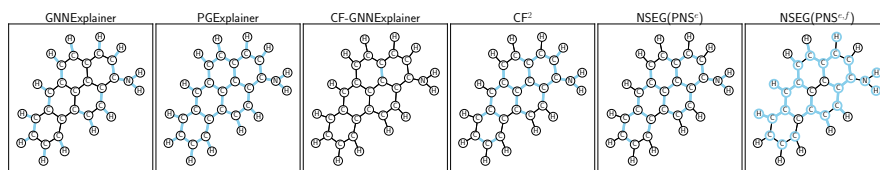
- [1] Alvarez-Melis, D., Jaakkola, T.S., 2017. A causal framework for explaining the predictions of black-box sequence-to-sequence models, in: EMNLP, Association for Computational Linguistics. pp. 412–421.
- [2] Amara, K., Ying, R., Zhang, Z., Han, Z., Shan, Y., Brandes, U., Schemm, S., Zhang, C., 2022. Graphframex: Towards systematic evaluation of explainability methods for graph neural networks. URL: <https://arxiv.org/abs/2206.09677>, doi:10.48550/ARXIV.2206.09677.
- [3] Arrieta, A.B., Rodríguez, N.D., Ser, J.D., Bennetot, A., Tabik, S., Barbado, A., García, S., Gil-Lopez, S., Molina, D., Benjamins, R., Chatila, R., Herrera, F., 2020. Explainable artificial intelligence (XAI): concepts, taxonomies, opportunities and challenges toward responsible AI. *Inf. Fusion* 58, 82–115.
- [4] Baldassarre, F., Azizpour, H., 2019. Explainability techniques for graph convolutional networks. doi:10.48550/ARXIV.1905.13686, arXiv:1905.13686.
- [5] Bareinboim, E., Forney, A., Pearl, J., 2015. Bandits with unobserved confounders: A causal approach, in: Advances in Neural Information Processing Systems, pp. 1342–1350. URL: <https://proceedings.neurips.cc/paper/2015/hash/795c7a7a5ec6b460ec00c5841019b9e9-Abstract.html>.
- [6] Beckers, S., 2022. Causal explanations and XAI, in: 1st Conference on Causal Learning and Reasoning, CLear 2022, PMLR. pp. 90–109.
- [7] Bruna, J., Zaremba, W., Szlam, A., LeCun, Y., 2014. Spectral networks and locally connected networks on graphs, in: ICLR.
- [8] Chattopadhyay, A., Manupriya, P., Sarkar, A., Balasubramanian, V.N., 2019. Neural network attributions: A causal perspective, in: ICML, PMLR. pp. 981–990.
- [9] Chen, M., Wei, Z., Ding, B., Li, Y., Yuan, Y., Du, X., Wen, J., 2020. Scalable graph neural networks via bidirectional propagation, in: NeurIPS.
- [10] Chen, X., Cai, R., Fang, Y., Wu, M., Li, Z., Hao, Z., 2023. Motif graph neural network. *IEEE Transactions on Neural Networks and Learning Systems*, 1–15doi:10.1109/TNNLS.2023.3281716.
- [11] Dou, Y., Shu, K., Xia, C., Yu, P.S., Sun, L., 2021. User preference-aware fake news detection, in: SIGIR, ACM. pp. 2051–2055.
- [12] Fan, W., Ma, Y., Li, Q., He, Y., Zhao, Y.E., Tang, J., Yin, D., 2019. Graph neural networks for social recommendation, in: The World Wide Web Conference, ACM. pp. 417–426. doi:10.1145/3308558.3313488.

- [13] Galhotra, S., Pradhan, R., Salimi, B., 2021. Explaining black-box algorithms using probabilistic contrastive counterfactuals, in: SIGMOD '21: International Conference on Management of Data, ACM. pp. 577–590. URL: <https://doi.org/10.1145/3448016.3458455>, doi:10.1145/3448016.3458455.
- [14] Gilmer, J., Schoenholz, S.S., Riley, P.F., Vinyals, O., Dahl, G.E., 2017. Neural message passing for quantum chemistry, in: ICML, PMLR. pp. 1263–1272.
- [15] Hamilton, W.L., Ying, Z., Leskovec, J., 2017. Inductive representation learning on large graphs, in: Advances in Neural Information Processing Systems, pp. 1024–1034.
- [16] Huang, C., Xu, H., Xu, Y., Dai, P., Xia, L., Lu, M., Bo, L., Xing, H., Lai, X., Ye, Y., 2021. Knowledge-aware coupled graph neural network for social recommendation, in: AAAI Conference on Artificial Intelligence, AAAI Press. pp. 4115–4122.
- [17] Huang, Q., Yamada, M., Tian, Y., Singh, D., Yin, D., Chang, Y., 2020. Graphlime: Local interpretable model explanations for graph neural networks. URL: <https://arxiv.org/abs/2001.06216>, doi:10.48550/ARXIV.2001.06216, arXiv:2001.06216.
- [18] Jung, Y., Kasiviswanathan, S.P., Tian, J., Janzing, D., Blöbaum, P., Bareinboim, E., 2022. On measuring causal contributions via do-interventions, in: ICML, PMLR. pp. 10476–10501.
- [19] Kingma, D.P., Welling, M., 2014. Auto-encoding variational bayes, in: ICLR.
- [20] Kipf, T.N., Welling, M., 2017. Semi-supervised classification with graph convolutional networks, in: International Conference on Learning Representations, OpenReview.net.
- [21] Klicpera, J., Bojchevski, A., Günnemann, S., 2019. Predict then propagate: Graph neural networks meet personalized pagerank, in: ICLR (Poster), OpenReview.net.
- [22] LeCun, Y., Bottou, L., Bengio, Y., Haffner, P., 1998. Gradient-based learning applied to document recognition. Proc. IEEE 86, 2278–2324. doi:10.1109/5.726791.
- [23] Lin, W., Lan, H., Li, B., 2021. Generative causal explanations for graph neural networks, in: International Conference on Machine Learning, PMLR. pp. 6666–6679.
- [24] Liu, M., Gao, H., Ji, S., 2020. Towards deeper graph neural networks, in: KDD, ACM. pp. 338–348.

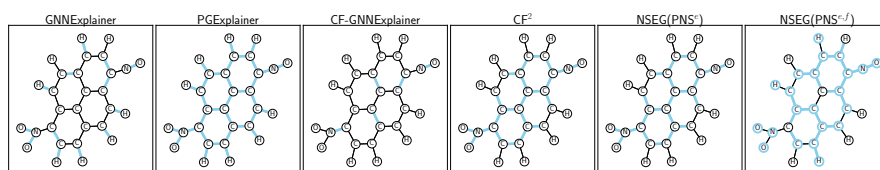
- [25] Lucic, A., ter Hoeve, M.A., Tolomei, G., de Rijke, M., Silvestri, F., 2022. Cf-gnnexplainer: Counterfactual explanations for graph neural networks, in: AISTATS, PMLR. pp. 4499–4511.
- [26] Lundberg, S.M., Lee, S., 2017. A unified approach to interpreting model predictions, in: Advances in Neural Information Processing Systems, pp. 4765–4774.
- [27] Luo, D., Cheng, W., Xu, D., Yu, W., Zong, B., Chen, H., Zhang, X., 2020. Parameterized explainer for graph neural network, in: Advances in Neural Information Processing Systems.
- [28] Magister, L.C., Kazhdan, D., Singh, V., Liò, P., 2021. Gcexplainer: Human-in-the-loop concept-based explanations for graph neural networks. URL: <https://arxiv.org/abs/2107.11889>, arXiv:2107.11889.
- [29] Microsoft, 2017. Image understanding. <https://www.microsoft.com/en-us/research/project/image-understanding>. Accessed: 2022-08-01.
- [30] Molnar, C., 2022. Interpretable Machine Learning. 2 ed. URL: <https://christophm.github.io/interpretable-ml-book>.
- [31] Morris, C., Kriege, N.M., Bause, F., Kersting, K., Mutzel, P., Neumann, M., 2020. Tudataset: A collection of benchmark datasets for learning with graphs arXiv:2007.08663.
- [32] Pearl, J., 1999. Probabilities of causation: Three counterfactual interpretations and their identification. Synth. 121, 93–149. doi:10.1023/A:1005233831499.
- [33] Pearl, J., 2009. Causality: Models, Reasoning and Inference. 2nd ed., Cambridge University Press, USA.
- [34] Pfeifer, B., Saranti, A., Holzinger, A., 2022. GNN-SubNet: disease subnetwork detection with explainable graph neural networks. Bioinformatics 38, ii120–ii126. URL: <https://doi.org/10.1093/bioinformatics/btac478>, doi:10.1093/bioinformatics/btac478, arXiv:https://academic.oup.com/bioinformatics/article-pdf/38/Supplement_2/ii120/49886271
- [35] Pope, P.E., Kolouri, S., Rostami, M., Martin, C.E., Hoffmann, H., 2019. Explainability methods for graph convolutional neural networks, in: IEEE Conference on Computer Vision and Pattern Recognition, Computer Vision Foundation / IEEE. pp. 10772–10781. doi:10.1109/CVPR.2019.01103.
- [36] Ribeiro, M.T., Singh, S., Guestrin, C., 2016. "why should I trust you?": Explaining the predictions of any classifier, in: International Conference on Knowledge Discovery and Data Mining, ACM. pp. 1135–1144. doi:10.1145/2939672.2939778.

- [37] Schölkopf, B., Locatello, F., Bauer, S., Ke, N.R., Kalchbrenner, N., Goyal, A., Bengio, Y., 2021. Towards causal representation learning. URL: <https://arxiv.org/abs/2102.11107>, arXiv:2102.11107.
- [38] Shan, C., Shen, Y., Zhang, Y., Li, X., Li, D., 2021. Reinforcement learning enhanced explainer for graph neural networks, in: Advances in Neural Information Processing Systems, Curran Associates, Inc.. pp. 22523–22533. URL: https://proceedings.neurips.cc/paper_files/paper/2021/file/be26abe76fb5c8a4921cf9d3e865b454-Paper.pdf.
- [39] Shi, C., Xu, M., Zhu, Z., Zhang, W., Zhang, M., Tang, J., 2020. Graphaf: a flow-based autoregressive model for molecular graph generation, in: International Conference on Learning Representations, OpenReview.net.
- [40] Sun, M., Zhao, S., Gilvary, C., Elemento, O., Zhou, J., Wang, F., 2020. Graph convolutional networks for computational drug development and discovery. *Briefings Bioinform.* 21, 919–935.
- [41] Sundararajan, M., Taly, A., Yan, Q., 2017. Axiomatic attribution for deep networks, in: Proceedings of the 34th International Conference on Machine Learning, PMLR. pp. 3319–3328. URL: <http://proceedings.mlr.press/v70/sundararajan17a.html>.
- [42] Tan, J., Geng, S., Fu, Z., Ge, Y., Xu, S., Li, Y., Zhang, Y., 2022. Learning and evaluating graph neural network explanations based on counterfactual and factual reasoning, in: The ACM Web Conference, ACM. pp. 1018–1027. doi:10.1145/3485447.3511948.
- [43] Tian, J., Pearl, J., 2000. Probabilities of causation: Bounds and identification, in: Conference in Uncertainty in Artificial Intelligence, Morgan Kaufmann. pp. 589–598.
- [44] Velickovic, P., Cucurull, G., Casanova, A., Romero, A., Liò, P., Bengio, Y., 2018. Graph attention networks, in: International Conference on Learning Representations, OpenReview.net.
- [45] Vu, M.N., Thai, M.T., 2020. Pgm-explainer: Probabilistic graphical model explanations for graph neural networks, in: Advances in Neural Information Processing Systems.
- [46] Wang, X., Wu, Y., Zhang, A., Feng, F., He, X., Chua, T.S., 2022. Reinforced causal explainer for graph neural networks. *IEEE Transactions on Pattern Analysis and Machine Intelligence*, 1–1doi:10.1109/TPAMI.2022.3170302.
- [47] Watson, D.S., Gultchin, L., Taly, A., Floridi, L., 2021. Local explanations via necessity and sufficiency: unifying theory and practice, in: Thirty-Seventh Conference on Uncertainty in Artificial Intelligence, AUAI Press. pp. 1382–1392.

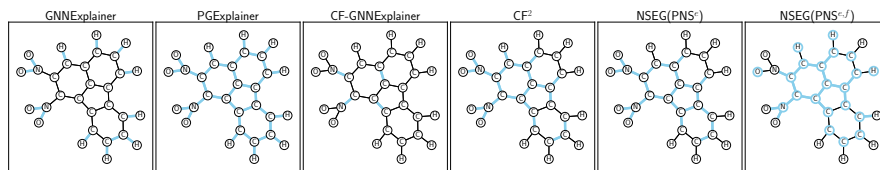
- [48] Wu, F., Jr., A.H.S., Zhang, T., Fifty, C., Yu, T., Weinberger, K.Q., 2019. Simplifying graph convolutional networks, in: ICML, PMLR. pp. 6861–6871.
- [49] Xu, B., Shen, H., Sun, B., An, R., Cao, Q., Cheng, X., 2021. Towards consumer loan fraud detection: Graph neural networks with role-constrained conditional random field, in: AAAI, AAAI Press. pp. 4537–4545.
- [50] Xu, K., Hu, W., Leskovec, J., Jegelka, S., 2019. How powerful are graph neural networks?, in: International Conference on Learning Representations, OpenReview.net.
- [51] Yang, M., Liu, F., Chen, Z., Shen, X., Hao, J., Wang, J., 2021. Causalvae: Disentangled representation learning via neural structural causal models, in: IEEE Conference on Computer Vision and Pattern Recognition, CVPR 2021, Computer Vision Foundation / IEEE. pp. 9593–9602. URL: https://openaccess.thecvf.com/content/CVPR2021/html/Yang_CausalVAE_Disentangled_Representation_Learning_via_Neural_Structural_Causal_Models_CVPR_2021_paper.html.
- [52] Ying, Z., Bourgeois, D., You, J., Zitnik, M., Leskovec, J., 2019. Gnnexplainer: Generating explanations for graph neural networks, in: Advances in Neural Information Processing Systems, pp. 9240–9251.
- [53] Yuan, H., Yu, H., Gui, S., Ji, S., 2020. Explainability in graph neural networks: A taxonomic survey. doi:10.48550/ARXIV.2012.15445, arXiv:2012.15445.
- [54] Zeiger, E., Ashby, J., Bakale, G., Enslein, K., Klopman, G., Rosenkranz, H., 1996. Prediction of salmonella mutagenicity. Mutagenesis 11, 471–484.
- [55] Zeng, H., Zhou, H., Srivastava, A., Kannan, R., Prasanna, V.K., 2020. Graphsaint: Graph sampling based inductive learning method, in: ICLR, OpenReview.net.
- [56] Zhang, M., Chen, Y., 2018. Link prediction based on graph neural networks, in: Advances in Neural Information Processing Systems, pp. 5171–5181. URL: <https://proceedings.neurips.cc/paper/2018/hash/53f0d7c537d99b3824f0f99d62ea2428-Abstract.html>.
- [57] Zhang, W., Wu, T., Wang, Y., Cai, Y., Cai, H., 2023. Towards trustworthy explanation: On causal rationalization, in: International Conference on Machine Learning, ICML 2023, PMLR. pp. 41715–41736.
- [58] Zhao, H., des Combes, R.T., Zhang, K., Gordon, G.J., 2019. On learning invariant representations for domain adaptation, in: Proceedings of the 36th International Conference on Machine Learning, ICML 2019, PMLR. pp. 7523–7532. URL: <http://proceedings.mlr.press/v97/zhao19a.html>.



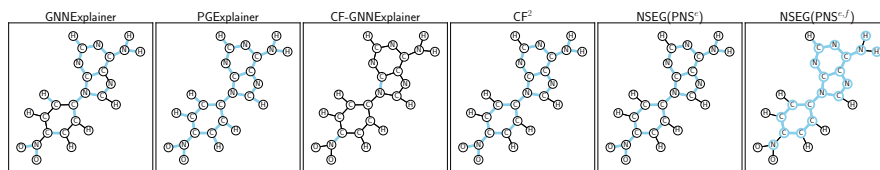
(a)



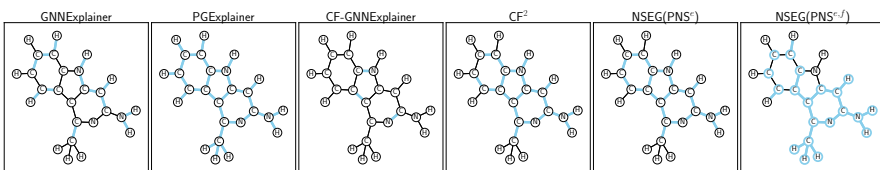
(b)



(c)

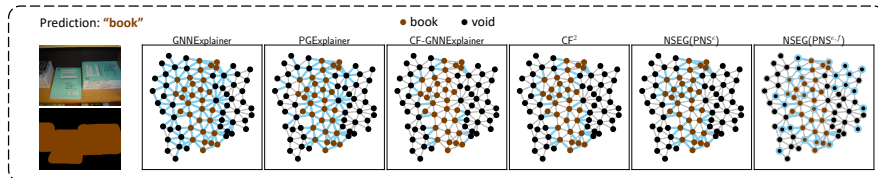


(d)

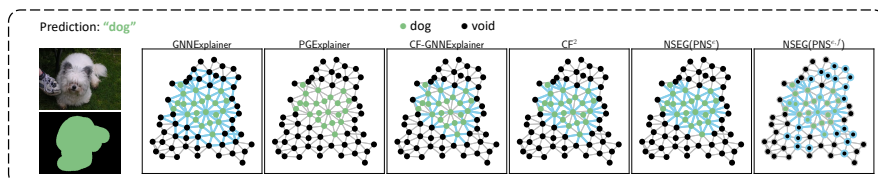


(e)

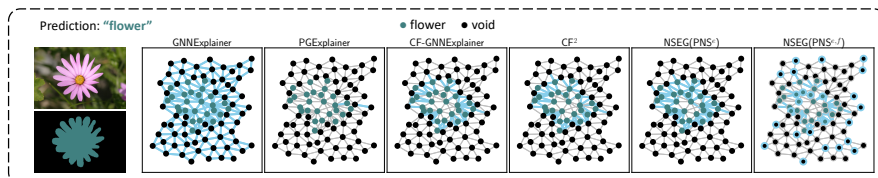
Figure C.8: Explanations of GNNExplainer, PGExplainer, CF-GNNExplainer, CF^2 , NSEG(PNS^e), and NSEG(PNS^{e,f}) on various Mutagenicity instances obtained by threshold, where the explanations are highlighted in blue.



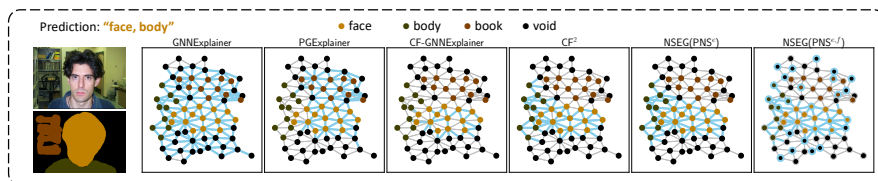
(a)



(b)



(c)



(d)

Figure C.9: Explanations of GNNExplainer, PGExplainer, CF-GNNExplainer, CF^2 , $NSEG(PNS^e)$, and $NSEG(PNS^{e,f})$ on various MSRC.21 instances obtained by threshold, where the explanations are highlighted in blue.